We are IntechOpen, the world's leading publisher of Open Access books Built by scientists, for scientists

4,800
Open access books available

122,000
International authors and editors

135M
Downloads

Our authors are among the

154
Countries delivered to

TOP 1%
most cited scientists

12.2%
Contributors from top 500 universities

CLARIVATE ANALYTICS BOOK CITATION INDEX INDEXED

WEB OF SCIENCE™

Selection of our books indexed in the Book Citation Index in Web of Science™ Core Collection (BKCI)

Interested in publishing with us?
Contact book.department@intechopen.com

Numbers displayed above are based on latest data collected.
For more information visit www.intechopen.com

5

Prediction of Partition Coefficients and Permeability of Drug Molecules in Biological Systems with Abraham Model Solute Descriptors Derived from Measured Solubilities and Water-to-Organic Solvent Partition Coefficients

William E. Acree, Jr.[1], Laura M. Grubbs[1] and Michael H. Abraham[2]
[1]*University of North Texas,*
[2]*University College London,*
[1]*United States*
[2]*United Kingdom*

1. Introduction

Modern drug testing and design includes experimental *in vivo* and *in vitro* measurements, combined with *in silico* computations that enable prediction of the drug candidate's ADMET (adsorption, distribution, metabolism, elimination and toxicity) properties in the early stages of drug discovery. Recent estimates place the discovery and development cost of a small drug molecule close to US $1.3 billion, from the time of inception to the time when the drug finally reaches the market place. Only 20 % of conceived drug candidates proceed to clinical trial stage testing, and of the compounds that enter clinical development less than 10 % receive government approval. Reasons for the low success rate include unsatisfactory efficacy, poor solubility, poor bioavailability, unfavorable pharmacokinetic properties, toxicity concerns and drug-drug interactions, degradation and poor shelf-life stability. Unfavorable pharmacokinetic and ADME properties, toxicity and adverse side effects account for up to two-thirds of drug failures. Traditional ADME analyses relied heavily on whole animal assays and the more labor intensive biochemical studies. High throughput screening methods, fast ADMET profiling assays, and computational approaches have allowed the pharmaceutical industry to identify quickly the less promising drug candidates in the very early development stage so that time and valuable resources are not spent pursuing compounds that have little probability of reaching the general population.

Of the fore-mentioned properties, the drug's aqueous solubility will likely be one of the first properties measured. Aqueous solubility is a major indicator of the drug's solubility in physiological gastrointestinal fluids and is a major indicator of the drug's oral bioavailability. Approximately 40 % of the proposed new pharmaceutical candidates are rejected in the very early stages of drug discovery because of their poor aqueous solubility resulting in bioavailability problems (Lukyanov and Torchilin, 2004; Keck *et al.*, 2008). The

number of failures due to poor solubility is likely to increase in future years because the new drug candidates generally have higher molecular weights and more complicated molecular structures than their predecessors. Moreover, drug molecules that are insoluble in water are difficult to study with existing *in vitro* biological assays, often give unreliable biological test results, and may precipitate from solution during storage or upon dilution. The importance of aqueous solubility in drug design is further evidenced by the fact that the editors of one prominent computational journal (Llinàs *et al*., 2008) challenged readers to develop *in silico* methods to predict the intrinsic solubilities of 32 crystalline drug like molecules in water from an experimental data set of accurately measured solubilities of 100 compounds. Only a few of the more successful approaches were actually published (Wang, *et al*. 2009; Hewitt *et al*., 2009). Similar challenges have been published regarding the prediction and measurement of the hydration free energies of functionally diverse neutral drug-like molecules (Nicholls *et al*., 2008; Guthrie, 2009). Aqueous solubility is the reference media to predict the absorption and bioavailability of orally administered drugs. More than 85 % of the drugs sold in the US and in Europe are administered orally.

Amidon and coworkers (1995) proposed a biopharmaceutical classification scheme (BCS) to categories drugs and drug candidates into four groups based on their combined solubility and permeability properties. The classification scheme is depicted in Figure 1a. Drug candidates in Class I exhibit high solubility and high permeability, which is preferred from both a bioavailability and drug delivery standpoint. A drug candidate is considered highly soluble when the highest dose strength is soluble in 250 ml water over a pH range 1 to 7.5. A drug candidate possesses high permeability when the extent of absorption in humans is determined to be 90% of an administered dose, based on the mass balance or in comparison to an intravenous dose. Drug candidates in Class II have low solubility and high permeability, hence, the dissolution rate becomes the governing parameter for bioavailability. These drugs exhibit variable bioavailability and need enhancement in the dissolution rate for improvement in bioavailability. Drug candidates in Class III have high solubility and low permeability. Permeation through the intestinal membrane represents the rate-determining step for Class III drug candidates, with the bioavailability being independent of drug release from the dosage form. Class IV drug candidates possess both low solubility and low permeability. Drugs in this category are generally not suitable for oral drug delivery unless one employs a special drug delivery technology (such as a nano-suspension). Wu and Benet (2005) examined the biopharmaceutical classification scheme as a predictive method for assessing drug disposition. The authors found that drugs in Classes I and II of BCS were metabolized and eliminated. Drugs in the latter two classes were eliminated unchanged from the body by renal and/or biliary elimination. On the basis of these findings the authors suggested the Biopharmaceutics Drug Disposition Classification System (BDDCS) where the extent of metabolism has replaced permeability as a classification criterion (see Figure 2b). Aqueous solubility is an important consideration in both drug classification systems. Adverse drug solubility can sometimes be overcome by structural modifications (e.g., prodrugs) or by adding an organic cosolvent, surfactant, hydrophilic macromolecular and/or an inclusion host compound (such as a modified cyclodextrin) to the drug formulation or application vehicle. Knowledge of the drug's solubility in different organic solvents aids in the selection of an appropriate organic cosolvent and provides valuable information regarding drug's molecular interactions with other organic molecules.

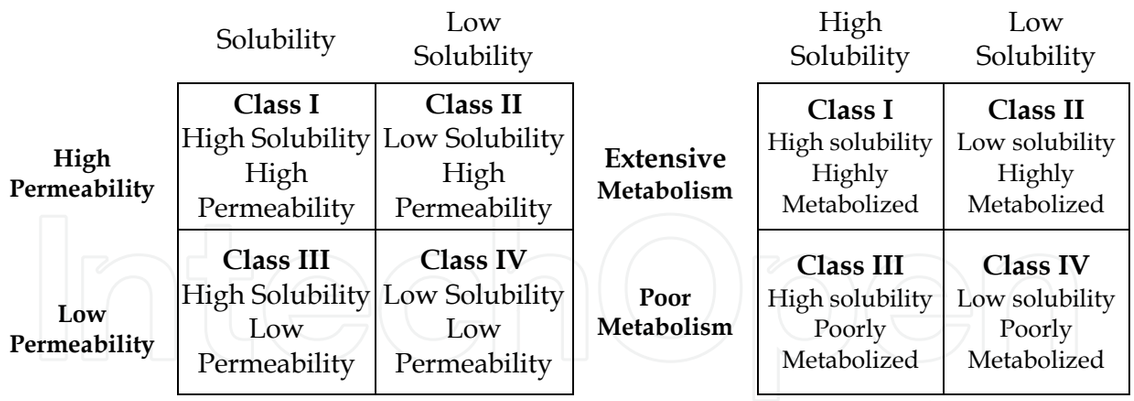

Fig. 1. Properties used in the Biopharmaceutical Classification Scheme (a) and Biopharmaceutics Drug Disposition Classification System (b)

Lipophilicity is another of the physical properties that is measured in the early stages of drug testing to predict the transport of molecules from the gastrointestinal track into the epithelial cells that line the inner and outer surfaces of the body. Most common drugs cross cellular barriers by transcellular pathways (across epithelial cells) that require the drug to enter the outer portion of the lipid bilayer of the cell membrane. The drug then diffuses to the inner lipid layer and travels across the cell before crossing the cell membrane once again to exit. Lipophilicity was introduced to describe a compound's affinity to be in lipid-like environment. Several solvent systems have been suggested as a surrogate to represent the lipid membrane against water. For convenience and economical reasons, the partition coefficient of the drug candidate between 1-octanol and a series of aqueous buffers has become the standard measure of lipophilicity. The *intrinsic lipophilicity* (logarithm of the water-to-octanol partition coefficient, log $P_{o/w}$) describes the equilibrium distribution of molecular drug candidate (unionized form of the molecule) between water and the aqueous buffer, and is independent of pH. The *effective lipophilicity* (logarithm of the water-to-octanol distribution coefficient) reflects the concentration ratio of the neutral drug molecule plus all ionized forms that may be present in the aqueous buffered solution at the given pH. The effective lipophilicity is often quoted at the physiological pH of 7.4. The intrinsic and effective lipophilicities are equivalent if the drug candidate contains no ionizable or protonatable functional groups. Experimental techniques employed to measure water-to-octanol partition coefficients include the traditional shake-flask method, as well as several methods based on reversed-phase liquid chromatography (hplc), counter-current chromatography and centrifugal partition chromatography (Sangster, 1989; Berthod *et al*., 1992; Menges *et al*., 1990; Berthod *et al*., 1988; McDuffie, 1981; Veith *et al*., 1979). Ribeiro and coworkers (2010) recently discussed the advantages and limitations associated with using the water-to-octanol partitioning system as a surrogate for biological membranes. The authors noted that there is a considerable difference between the homogeneous macroscopic 1-octanol solvent system and the highly-ordered microscopic structure of a lipid layer. Chromatographic retention data determined using an immobilized artificial membrane (IAM) stationary phase was suggested as a more appropriate method for measuring the lipophilicity of drug candidates and for quantifying drug-membrane interactions.

Solubility and water-to-organic solvent partition coefficients are fairly easy to measure as the equilibrated solutions contain only the dissolved drug candidate and the solubilizing solvent media. Blood-to-tissue partition coefficients, plasma-to-milk partition coefficient, percentage of human intestinal absorption and the steady-state volume of distribution are much harder to measure. The analytical methodology employed to measure these latter properties must be able to distinguish and quantify the drug from all of the many other molecules present in the biological sample. It is not easy, even with today's modern instrumentation, to design chemical analysis methods that are specific to a given molecule. Moreover, measurements involving human and/or animal tissues are expensive and are subject to larger experimental uncertainties. Replicate studies involving the same animal species have shown that the measured values can depend on gender, age and eating habits. This chapter will discuss the prediction of the blood-to-tissue partition coefficients, plasma-to-milk partition coefficients, human intestinal absorption based on the Abraham solvation parameter model and solute descriptors calculated from measured solubilities and partition coefficients.

2. Abraham solvation parameter model

The Abraham general solvation model is one of the more useful approaches for the analysis and prediction of the adsorption, distribution and toxicological properties of potential drug candidates. The method relies on two linear free energy relationships (lfers), one for transfer processes occurring within condensed phases (Abraham, 1993a,b; Abraham *et al*., 2004):

$$SP = c + e \cdot \mathbf{E} + s \cdot \mathbf{S} + a \cdot \mathbf{A} + b \cdot \mathbf{B} + v \cdot \mathbf{V} \quad (1)$$

and one for processes involving gas-to-condensed phase transfer

$$SP = c + e \cdot \mathbf{E} + s \cdot \mathbf{S} + a \cdot \mathbf{A} + b \cdot \mathbf{B} + l \cdot \mathbf{L} \quad (2)$$

The dependent variable, SP, is some property of a series of solutes in a fixed phase, which in the present study will include the logarithm of drug's water-to-organic solvent and blood-to-tissue partition coefficients, the logarithm of the drug's molar solubility in an organic solvent divided by its aqueous molar solubility, the logarithm of the drug's plasma-to-milk partition coefficient, percent human intestinal absorption and the logarithm of the kinetic constant for human intestinal absorption, and the logarithm of the human skin permeability coefficient. The independent variables, or descriptors, are solute properties as follows: **E** and **S** refer to the excess molar refraction and dipolarity/polarizability descriptors of the solute, respectively, **A** and **B** are measures of the solute hydrogen-bond acidity and basicity, **V** is the McGowan volume of the solute and **L** is the logarithm of the solute gas phase dimensionless Ostwald partition coefficient into hexadecane at 298 K. The first four descriptors can be regarded as measures of the tendency of the given solute to undergo various solute-solvent interactions. The latter two descriptors, **V** and **L**, are both measures of solute size, and so will be measures of the solvent cavity term that will accommodate the dissolved solute. General dispersion interactions are also related to solute size, hence, both **V** and **L** will also describe the general solute-solvent interactions. Solute descriptors are available for more than 4,000 organic, organometallic and inorganic solutes. No single article lists all of the numerical values; however, a large compilation is available in one published review article (Abraham *et al*., 1993a), and in the supporting material that has accompanied

several of our published papers (Abraham *et al*., 2006a; Abraham *et al*., 2009a; Mintz *et al*., 2007). Solute descriptors can be obtained by regression analysis using various types of experimental data, including water-to-solvent partitions, gas-to-solvent partitions, solubility data and chromatographic retention data as discussed below and elsewhere (Abraham *et al*., 2010; Zissimos *et al*., 2002a,b). For a number of partitions into solvents that contain large amounts of water at saturation, an alternative hydrogen bond basicity parameter, $\mathbf{B^o}$, is used for specific classes of solute: alkylpyridines, alkylanilines, and sulfoxides.

Equations 1 and 2 contain the following three quantities: (a) measured solute properties; (b) calculated solute descriptors; and (c) calculated equation coefficients. Knowledge of any two quantities permits calculation of the third quantity through the solving of simultaneous equations and regression analysis. Solute descriptors are calculated from measured partition coefficient ($P_{solute,system}$), chromatographic retention factor (k') and molar solubility ($C_{solute,solvent}$) data for the solutes dissolved in partitioning systems and in organic solvents having known equation coefficients. Generally partition coefficient, chromatographic retention factor and molar solubility measurements are fairly accurate, and it is good practice to base the solute descriptor computations on observed values having minimal experimental uncertainty. The computation is depicted graphically in Figure 1 by the unidirectional arrows that indicate the direction of the calculation using the known equation coefficients that connect the measured and solute descriptors. Measured $P_{solute,system}$ and $C_{solute,solvent}$ values yield solute descriptors. The unidirectional red arrows originating from the center solute descriptor circle represent the equation coefficients that have been reported for blood-to-brain partition coefficient, blood-to-tissue partition coefficients, percentage of human intenstinal absorption, Draize eye scores, and aquatic toxicity Abraham model linear free energy relationships. Plasma-to-milk partition ratio predictions are achieved (Abraham *et al*., 2009b) through an artificial neural network with five inputs, 14 nodes in the hidden layer and one node in the output layer. Linear analysis of the plasma-to-milk partition ratios for 179 drugs and hydrophobic environmental pollutants revealed that drug molecules preferentially partition into the aqueous and protein phases of milk. Hydrophobic environmental pollutants, on the other hand, partition into the fat phase. Prediction of the fore-mentioned ADMET and biological properties does require a prior knowledge of the Abraham solute descriptors for the drug candidate of interest. There are also commercial software packages (ADME Boxes, 2010) and several published estimation schemes (Mutelet and Rogalski, 2001; Arey *et al*., 2005; Platts *et al*., 1999; Abraham and McGowan, 1987) for calculating the numerical values of solute descriptors from molecular structural information if one is unable to find the necessary partition, chromatographic and/or solubility data. For any fully characterized system/process (those with calculated values for the equation coefficients) further values of SP can be estimated for solutes with known values for the solute descriptors.

The usefulness of Eqns. 1 and 2 in the characterization of solvent phases is that the coefficients *e, s, a, b, l* and *v* are not just curve-fitting constants. The coefficients reflect particular solute-solvent interactions that correspond to chemical properties of the solvent phase. The excess molar refraction, **E**, is defined from the solute refractive index, and hence the *e* coefficient gives a measure of general solute-solvent dispersion interactions. The **V** and **L** descriptors were set up as measures of the endoergic effect of disrupting solvent-solvent bonds. However, solute volume is always well correlated with polarizability and so the *v* and *l* coefficients will include not only an endoergic cavity effect but also exoergic solute-

solvent effects that arise through solute polarizability. The **S** descriptor is a measure of dipolarity and polarizability and hence the *s* coefficient will reflect the ability of a solvent to undergo dipole-dipole and dipole-induced dipole interactions with the solute. The **A** descriptor is a measure of solute hydrogen bond acidity, and hence the *a* coefficient will reflect the complementary solvent hydrogen bond basicity. Similarly the *b* coefficient will be a measure of solvent hydrogen bond acidity. All this is straightforward for gas-to-solvent partitions because there are no interactions to consider in the gas phase. For partition between solvents, the coefficients in Eqn. 1 then refer to differences between the properties of the two phases.

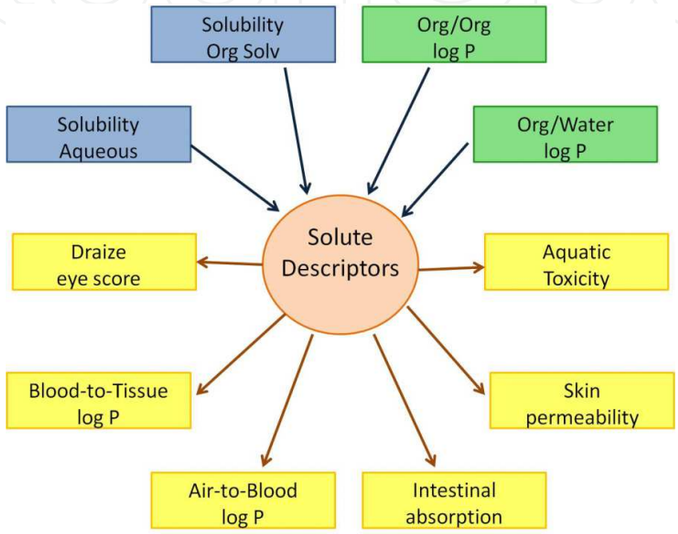

Fig. 2. Outline illustrating the calculation of Abraham model solute descriptors from experimental partition coefficient and solubility data, and then using the calculated values to estimate biological activities and partitioning, such as blood-to-tissue partition coefficients, Draize eye scores, aquatic toxicities and air-to-blood partition coefficients.

The Abraham model equation coefficients encode chemical information, and several methods have been suggested to assess the chemical similarity between different partitioning processes/systems. Abraham and Martins (2004) calculated the five-dimensional distance between the coefficients as points in five-dimensional space by straightforward geometry

$$\text{Distance} = \sqrt{(e_i - e_j)^2 + (s_i - s_j)^2 + (a_i - a_j)^2 + (b_i - b_j)^2 + (v_i - v_j)^2} \quad (3)$$

where the subscripts "i" and "j" denote the two partitioning processes being compared. For comparison purposes, the authors suggested that for a good chemical model the calculated distance should be less than about 0.5 – 0.8. The water-to-isobutanol and water-to-octanol partitioning systems were the two chemical systems that the authors found closest to human skin permeability, with calculated distances of 1.2 and 1.9, respectively. The chemical interactions that govern skin permeability were quite different from the chemical interactions governing solute partitioning between water and isobutanol, and between water and 1-octanol. Ishiharma and Asakawa (1999) suggested a different comparison method based on calculating the cosine of the angle (cos θij) between the coefficients

$$Cos\ \Theta_{ij} = \frac{e_i e_j + s_i s_j + a_i a_j + b_i b_j + v_i v_j}{\sqrt{e_i^2 + s_i^2 + a_i^2 + b_i^2 + v_i^2}\ \sqrt{e_j^2 + s_j^2 + a_j^2 + b_j^2 + v_j^2}} \quad (4)$$

which are now regarded as lines in five-dimensional space. The angle between the two lines, θ_{ij}, yields information regarding how the two compared processes are in terms of their chemical similarity. As θ_{ij} approaches zero (or alternatively as cos θ_{ij} approaches unity) the two lines coincide, and the correlation between the two partitioning processes/systems approaches unity. Analysis of the Abraham model coefficients for the solubility of gases and vapors in biological phases (blood, brain, fat, heart, kidney, liver, lung and muscle) and organic solvents (alcohols, amides, olive oil, chloroform, diethyl ether, butanone), and equation coefficients for biological activity (nasal pungency thresholds, eye irritation thresholds, odor detection and anesthesia) using Eqns. 3 and 4 (along with Principal Component Analysis) found N-methylformamide to be an excellent model for both eye irritation thresholds in humans and nasal pungency thresholds in humans (Abraham *et al*., 2009a). The receptor site controlling both biological responses must be protein-like in character. The study further showed that no organic solvent is a suitable model (or surrogate) for blood, brain, heart, kidney, liver, lung and muscle. Two relatively nonpolar solvents (olive oil and chloroform) were found to be suitable models for fat, which is not too surprising given that fat is about 80 % lipid.

3. Experimental methods for measuring thermodynamic and kinetic solubilities

Recent advances in automated chemical synthesis and combinatorial chemistry have generated large numbers of new chemical compounds that need to be screened for possible biological activity and desired ADMET properties. The conventional experimental methods that were once used in the pharmaceutical industry to measure solubility and water-to-organic solvent partition coefficients are inadequate to handle large numbers of new compound because of low throughput capacity and the amount of compound required for the experimental determination. Large quantities of highly purified compounds are not usually available in the initial stages of drug discovery and drug testing. To meet the demands imposed by the increased compound numbers, the pharmaceutical industry has developed miniaturized and automated sample preparation platforms, combined with rapid chemical analysis methods based on nephelometric, uv/visible absorption and/or chromatographic measurements. The experimental protocol used depends on whether one needs to measure the kinetic or thermodynamic solubility.

High throughput kinetic aqueous solubility assays are based on the detection of precipitation of compounds in aqueous or aqueous buffered solutions. Typically, small known aliquots of the stock solution are added incrementally to the aqueous (or aqueous buffered solution) at predetermined time intervals until the solubility limit is reached. The resulting precipitation can be detected optically by nephlometric or laser monitoring methods, and the kinetic solubility is defined as the solute concentration immediately preceding the point at which precipitation was first detected. Kinetic solubility thus represents the maximum solubility of the fastest precipitation species of the given compound into the desired solubilizing solvent media. Numerous modifications of kinetic assays have been suggested in recent years. The suggested modifications differ in the dilution and detection method. For example, Lipinski *et al*. (2001) added small aliquots of a

stock solution of the drug (dissolved in dimethyl sulfoxide, DMSO) to the aqueous solvent media every minute until precipitation occurred. The DMSO in solution did increase with each added aliquot and may result in a higher measured aqueous solubility. Dimethyl sulfoxide is known to increase the solubility by helping to solvate the more lipophilic drug compounds. Solubility enhancement by dimethyl sulfoxide can be reduced if the samples are first serially diluted in dimethyl sulfoxide before the aliquots are added to the aqueous solvent system. Special 96-well plates have been designed to facilitate high throughput solubility measurements. The method depicted in Figure 3 allows one to quickly measure the aqueous solubility and aqueous-buffered solubility of 12 different drug candidates. The eight DMSO-diluted concentrations (1 mM to 100 mM) of each drug candidate are placed in the specified well of the drug's respective column. In the 12 x 9 cell matrix, the drug is identified by column number and the concentration is identified by row number. A predetermined aliquot volume from each of the DMSO diluted sample wells is transferred to the corresponding cell in the aqueous plate and aqueous-buffered plate. The volume of DMSO-diluted sample is the same for each transferred aliquot. Each cell in the aqueous plate and aqueous-buffered plate contains an identical volume of solvent. The cell contents are examined for precipitation immediately after the passage of the defined time interview, or alternatively, one can remove the solid and determine the concentration of dissolved drug by standard spectroscopic and/or chromatographic methods.

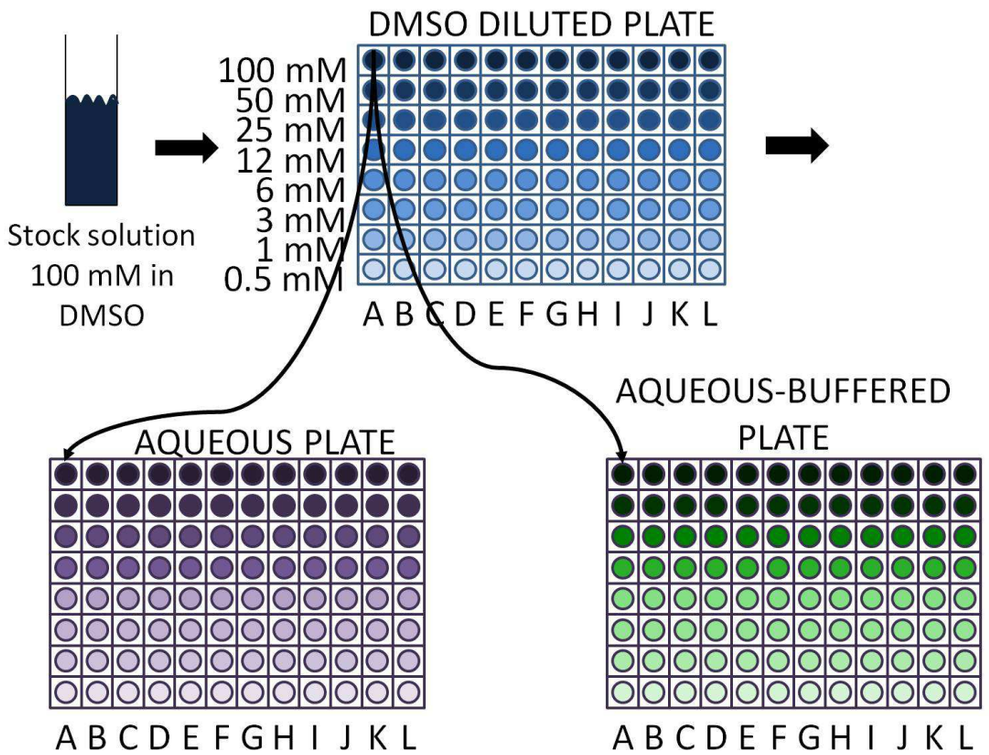

Fig. 3. Outline of a high throughput method for measuring drug solubility in water and in an aqueous-buffered solution using a 96-well plate.

Kinetic methods often overestimate the thermodynamic drug solubility because of the increased solubilization effect caused by the presence of dimethyl sulfoxide in the aqueous solvent and by the fact that one has not allowed sufficient time for equilibrium to be

achieved. Thermodynamic solubility is defined as the concentration in solution of a compound in equilibrium with an excess of solid material being present in solution at the conclusion of the dissolution process. Thermodynamic solubility is considered the "true" solubility of a compound. Experimental methods for determining thermodynamic solubility may be grouped into categories, one that extends the experimental protocols of exiting kinetic solubility determinations to longer "equilibration times" and the other that conducts solubility studies on solid compounds obtained from dried stock solutions to remove the enhancement effects caused by having the added dimethyl sulfoxide present in the final equilibrated solution. The rationale behind the longer equilibration times is that sufficient time will now be afforded for the first-precipitated crystalline phase to convert to the more thermodynamically stable crystalline phase. Sugano and coworkers (2006) reported a significant decrease in solubility with equilibration time for more than half of the 26 model compounds studied.

The preceding discussion focused on aqueous kinetic and thermodynamic solubility measurements. There is no reason that the basic high throughput experimental methodologies cannot be applied to organic solvents and to aqueous-organic solvent mixtures. Measured drug solubility in organic solvents, in combination with the Abraham general solvation model, provides valuable information in regarding the molecule's hydrogen-bonding character and dipolarity. Solubility ratios are substituted into Eqns. 1 and 2 to give the following mathematical correlations:

$$\log\left(C_{A,organic} / C_{A,water}\right) = c + e \cdot \mathbf{E} + s \cdot \mathbf{S} + a \cdot \mathbf{A} + b \cdot \mathbf{B} + v \cdot \mathbf{V} \quad (5)$$

$$\log\left(C_{A,organic} / C_{A,gas}\right) = c + e \cdot \mathbf{E} + s \cdot \mathbf{S} + a \cdot \mathbf{A} + b \cdot \mathbf{B} + l \cdot \mathbf{L} \quad (6)$$

where $C_{A,organic}$ and $C_{A,water}$ denote the molar solubility of the solute (component A) in the anhydrous "dry" organic solvent and in water, respectively, and $C_{A,gas}$ is the molar gas phase concentration of the solute above the crystalline phase at the system temperature. This later quantity is calculable as $C_{A,gas} = P_A^o V/RT$, from the solute's vapor pressure above the crystalline phase, P_A^o.

The solubility ratio in Eqn. 5 represents a hypothetical partitioning process for transferring the solute from water to the anhydrous organic solvent as depicted in Figure 4. Also depicted in Figure 4 are the gas-to-water and gas-to-organic solvent partitioning processes, along with their respective concentration ratios. The hypothetical water-to-organic solvent partitioning process should not be confused with the direct practical organic solvent/water partitioning system that corresponds to the equilibrium solute partitioning between a water-saturated organic phase and an aqueous phase saturated with the organic solvent. For solvents that are partially miscible with water, such as 1-butanol and ethyl acetate, partition coefficients calculated as the ratio of the molar solute solubilities in the organic solvent and water are not the same as those obtained from direct partition between water (saturated with the organic solvent) and organic solvent (saturated with water). Solubility ratios and practical partition coefficients, however, are nearly identical for solvents like linear alkanes, cycloalkanes, chloroform, carbon tetrachloride and dichloromethane, which are almost "completely" immiscible with water. Tables 1 and 2 give the equation coefficients for the Abraham model solubility ratio correlations (Eqns. 5 and 6) for the different organic solvents that have been reported to date.

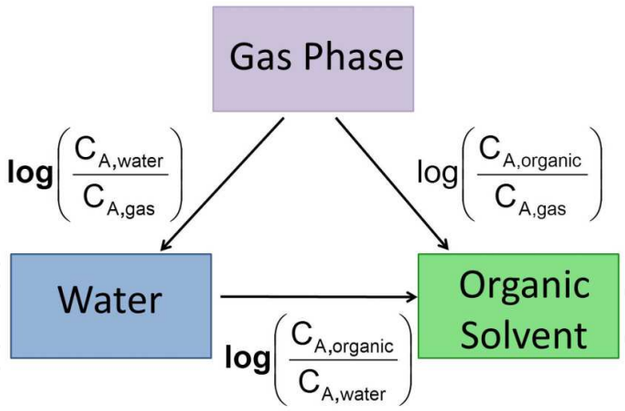

Fig. 4. Solubility ratios describing the various solute transfer processes.

Dry Solvent	c	e	s	a	b	v
Olely alcohol	-0.096	0.148	-0.841	-0.438	-4.040	4.125
Dichloromethane	0.319	0.102	-0.187	-3.058	-4.090	4.324
Trichloromethane	0.191	0.105	-0.403	-3.112	-3.514	4.395
Tetrachloromethane	0.199	0.523	-1.159	-3.560	-4.594	4.618
1,2-Dichloroethane	0.183	0.294	-0.134	-2.801	-4.291	4.180
1-Chlorobutane	0.222	0.273	-0.569	-2.918	-4.883	4.456
Butane	0.297	-0.005	-1.584	-3.188	-4.567	4.562
Pentane	0.369	0.386	-1.568	-3.535	-5.215	4.514
Hexane	0.361	0.579	-1.723	-3.599	-4.764	4.344
Heptane	0.325	0.670	-2.061	-3.317	-4.733	4.543
Octane	0.223	0.642	-1.647	-3.480	-5.067	4.526
Nonane	0.240	0.619	-1.713	-3.532	-4.921	4.482
Decane	0.160	0.585	-1.734	-3.435	-5.078	4.582
Undecane	0.058	0.603	-1.661	-3.421	-5.120	4.619
Dodecane	0.114	0.668	-1.664	-3.545	-5.006	4.459
Hexadecane	0.087	0.667	-1.617	-3.587	-4.869	4.433
Cyclohexane	0.159	0.784	-1.678	-3.740	-4.929	4.577
Methylcyclohexane	0.246	0.782	-1.982	-3.517	-4.293	4.528
Isooctane	0.318	0.555	-1.737	-3.677	-4.864	4.417
Benzene	0.142	0.464	-0.588	-3.099	-4.625	4.491
Toluene	0.143	0.527	-0.720	-3.010	-4.824	4.545
Fluorobenzene	0.139	0.152	-0.374	-3.030	-4.601	4.540
Chlorobenzene	0.065	0.381	-0.521	-3.183	-4.700	4.614
Bromobenzene	-0.017	0.436	-0.424	-3.174	-4.558	4.445
Iodobenzene	-0.192	0.298	-0.308	-3.213	-4.653	4.588
Nitrobenzene	-0.152	0.525	0.081	-2.332	-4.494	4.187
Benzonitrile	0.155	0.337	-0.036	-1.544	-4.614	3.990
Olive oil	-0.035	0.574	-0.798	-1.422	-4.984	4.210
Carbon disulfide	0.047	0.686	-0.943	-3.603	-5.818	4.921
Isopropyl myristate	-0.605	0.930	-1.153	-1.682	-4.093	4.249
Triolein	0.385	0.983	-2.083	-2.007	-3.452	4.072

Dry Solvent	c	e	s	a	b	v
Methanol	0.276	0.334	-0.714	0.243	-3.320	3.549
Ethanol	0.222	0.471	-1.035	0.326	-3.596	3.857
Propan-1-ol	0.139	0.405	-1.029	0.247	-3.767	3.986
Butan-1-ol	0.165	0.401	-1.011	0.056	-3.958	4.044
Pentan-1-ol	0.150	0.536	-1.229	0.141	-3.864	4.077
Hexan-1-ol	0.115	0.492	-1.164	0.054	-3.978	4.131
Heptan-1-ol	0.035	0.398	-1.063	0.002	-4.343	4.317
Octan-1-ol	-0.034	0.489	-1.044	-0.024	-4.235	4.218
Decan-1-ol	-0.058	0.616	-1.319	0.026	-4.153	4.279
Propan-2-ol	0.099	0.343	-1.049	0.406	-3.827	4.033
Isobutanol	0.127	0.253	-0.976	0.158	-3.882	4.114
sec-Butanol	0.188	0.354	-1.127	0.016	-3.568	3.968
tert-Butanol	0.211	0.171	-0.947	0.331	-4.085	4.109
3-Methyl-1-butanol	0.073	0.360	-1.273	0.090	-3.770	4.273
Pentan-2-ol	0.115	0.455	-1.331	0.206	-3.745	4.201
Ethylene glycol	-0.270	0.578	-0.511	0.715	-2.619	2.729
2,2,2 -Trifluoroethanol	0.395	-0.094	-0.594	-1.280	-1.274	3.088
Diethyl ether	0.350	0.358	-0.820	-0.588	-4.956	4.350
Tetrahydrofuran	0.207	0.372	-0.392	-0.236	-4.934	4.447
1,4-Dioxane	0.098	0.350	-0.083	-0.556	-4.826	4.172
Dibutyl ether	0.176	0.394	-0.985	-1.414	-5.357	4.524
Methyl *tert*-butyl ether	0.341	0.307	-0.817	-0.618	-5.097	4.425
Methyl acetate	0.351	0.223	-0.150	-1.035	-4.527	3.972
Ethyl acetate	0.328	0.369	-0.446	-0.700	-4.904	4.150
Butyl acetate	0.248	0.356	-0.501	-0.867	-4.973	4.281
Propanone	0.313	0.312	-0.121	-0.608	-4.753	3.942
Butanone	0.246	0.256	-0.080	-0.767	-4.855	4.148
Cyclohexanone	0.038	0.225	0.058	-0.976	-4.842	4.315
Dimethylformamide	-0.305	-0.058	0.343	0.358	-4.865	4.486
Dimethylacetamide	-0.271	0.084	0.209	0.915	-5.003	4.557
Diethylacetamide	0.213	0.034	0.089	1.342	-5.084	4.088
Dibutylformamide	0.332	0.302	-0.436	0.358	-4.902	3.952
N-Methylpyrolidinone	0.147	0.532	0.225	0.840	-4.794	3.674
N-Methyl-2-piperidone	0.056	0.332	0.257	1.556	-5.035	3.983
N-Formylmorpholine	-0.032	0.696	-0.062	0.014	-4.092	3.405
N-Methylformamide	0.114	0.407	-0.287	0.542	-4.085	3.471
N-Ethylformamide	0.220	0.034	-0.166	0.935	-4.589	3.730
N-Methylacetamide	0.090	0.205	-0.172	1.305	-4.589	3.833
N-Ethylacetamide	0.284	0.128	-0.442	1.180	-4.728	3.856
Formamide	-0.171	0.070	0.308	0.589	-3.152	2.432
Acetonitrile	0.413	0.077	0.326	-1.566	4.391	3.364
Nitromethane	0.023	-0.091	0.793	-1.463	-4.364	3.460
Dimethylsulfoxide	-0.194	0.327	0.791	-1.260	-4.540	3.361
Tributylphosphate	0.327	0.570	-0.837	-1.069	-4.333	3.919

Dry Solvent	c	e	s	a	b	v
Propylene carbonate	0.004	0.168	0.504	-1.283	-4.407	3.421
Gas-water	-0.994	0.577	2.549	3.813	4.841	-0.869

Table 1. Coefficients in Eqn. 5 for Correlating Solute Solubility in Dry Organic Solvents at 298 K

Dry Solvent	c	e	s	a	b	l
Olely alcohol	-0.268	-0.392	0.800	3.117	0.978	0.918
Dichloromethane	0.192	-0.572	1.492	0.460	0.847	0.965
Trichloromethane	0.157	-0.560	1.259	0.374	1.333	0.976
Tetrachloromethane	0.217	-0.435	0.554	0.000	0.000	1.069
1,2-Dichloroethane	0.017	-0.337	1.600	0.774	0.637	0.921
1-Chlorobutane	0.130	-0.581	1.114	0.724	0.000	1.016
Butane	0.291	-0.360	0.091	0.000	0.000	0.959
Pentane	0.335	-0.276	0.000	0.000	0.000	0.968
Hexane	0.292	-0.169	0.000	0.000	0.000	0.979
Heptane	0.275	-0.162	0.000	0.000	0.000	0.983
Octane	0.215	-0.049	0.000	0.000	0.000	0.967
Nonane	0.200	-0.145	0.000	0.000	0.000	0.980
Decane	0.156	-0.143	0.000	0.000	0.000	0.989
Undecane	0.113	0.000	0.000	0.000	0.000	0.971
Dodecane	0.053	0.000	0.000	0.000	0.000	0.986
Hexadecane	0.000	0.000	0.000	0.000	0.000	1.000
Cyclohexane	0.163	-0.110	0.000	0.000	0.000	1.013
Methylcyclohexane	0.319	-0.215	0.000	0.000	0.000	1.012
Isooctane	0.264	-0.230	0.000	0.000	0.000	0.975
Benzene	0.107	-0.313	1.053	0.457	0.169	1.020
Toluene	0.121	-0.222	0.938	0.467	0.099	1.012
Fluorobenzene	0.181	-0.621	1.432	0.647	0.000	0.986
Chlorobenzene	0.064	-0.399	1.151	0.313	0.171	1.032
Bromobenzene	-0.064	-0.326	1.261	0.323	0.292	1.002
Iodobenzene	-0.171	-0.192	1.197	0.245	0.245	1.002
Nitrobenzene	-0.275	0.001	1.861	1.119	0.000	0.925
Benzonitrile	-0.062	-0.402	1.939	2.007	0.000	0.880
Olive oil	-0.159	-0.277	0.904	1.695	-0.090	0.876
Carbon disulfide	0.101	0.251	0.177	0.027	0.095	1.068
Triolein	0.147	0.254	-0.246	1.520	1.473	0.918
Methanol	-0.039	-0.338	1.317	3.836	1.396	0.773
Ethanol	0.017	-0.232	0.867	3.894	1.192	0.846
Propan-1-ol	-0.042	-0.246	0.749	3.888	1.078	0.874
Butan-1-ol	-0.004	-0.285	0.768	3.705	0.879	0.890
Pentan-1-ol	-0.002	-0.161	0.535	3.778	0.960	0.900
Hexan-1-ol	-0.014	-0.205	0.583	3.621	0.891	0.913

Dry Solvent	c	e	s	a	b	l
Heptan-1-ol	-0.056	-0.216	0.554	3.596	0.803	0.933
Octan-1-ol	-0.147	-0.214	0.561	3.507	0.749	0.943
Decan-1-ol	-0.139	-0.090	0.356	3.547	0.727	0.958
Propan-2-ol	-0.048	-0.324	0.713	4.036	1.055	0.884
Isobutanol	-0.034	-0.387	0.719	3.736	1.088	0.905
sec-Butanol	-0.003	-0.357	0.699	3.595	1.247	0.881
tert-Butanol	0.053	-0.443	0.699	4.026	0.882	0.907
3-Methyl-1-butanol	-0.052	-0.430	0.628	3.661	0.932	0.937
Pentan-2-ol	-0.031	-0.325	0.496	3.792	1.024	0.934
Ethylene glycol	-0.887	0.132	1.657	4.457	2.355	0.565
2,2,2-Trifluoroethanol	-0.092	-0.547	1.339	2.213	3.807	0.645
Diethyl ether	0.288	-0.379	0.904	2.937	0.000	0.963
Tetrahydrofuran	0.189	-0.347	1.238	3.289	0.000	0.982
1,4-Dioxane	-0.034	-0.354	1.674	3.021	0.000	0.919
Dibutyl ether	0.153	-0.406	0.758	2.152	-0.610	1.008
Methyl *tert*-butyl ether	0.231	-0.536	0.890	2.623	0.000	0.999
Methyl acetate	0.129	-0.447	1.675	2.625	0.213	0.874
Ethyl acetate	0.182	-0.352	1.316	2.891	0.000	0.916
Butyl acetate	0.147	-0.414	1.212	2.623	0.000	0.954
Propanone	0.127	-0.387	1.733	3.060	0.000	0.866
Butanone	0.112	-0.474	1.671	2.878	0.000	0.916
Cyclohexanone	-0.086	-0.441	1.725	2.786	0.000	0.957
Dimethylformamide	-0.391	-0.869	2.107	3.774	0.000	1.011
Dimethylacetamide	-0.308	-0.736	1.802	4.361	0.000	1.028
Diethylacetamide	-0.075	-0.434	1.911	4.801	0.000	0.899
Dibutylformamide	-0.002	-0.239	1.402	4.029	0.000	0.900
N-Methylpyrolidinone	-0.128	-0.029	2.217	4.429	0.000	0.777
N-Methyl-2-piperidone	-0.264	-0.171	2.086	5.056	0.000	0.883
N-Formylmorpholine	-0.437	0.024	2.631	4.318	0.000	0.712
N-Methylformamide	-0.249	-0.142	1.661	4.147	0.817	0.739
N-Ethylformamide	-0.220	-0.302	1.743	4.498	0.480	0.824
N-Methylacetamide	-0.197	-0.175	1.608	4.867	0.375	0.837
N-Ethylacetamide	-0.018	-0.157	1.352	4.588	0.357	0.824
Formamide	-0.800	0.310	2.292	4.130	1.933	0.442
Acetonitrile	-0.007	-0.595	2.461	2.085	0.418	0.934
Nitromethane	-0.340	-0.297	2.689	2.193	0.514	0.728
Dimethylsulfoxide	-0.556	-0.223	2.903	5.036	0.000	0.719
Tributylphosphate	0.097	-0.098	1.103	2.411	0.588	0.844
Propylene carbonate	-0.356	-0.413	2.587	2.207	0.455	0.719
Gas-water	-1.271	0.822	2.743	3.904	4.814	-0.213

Table 2. Coefficients in Eqn. 6 for Correlating Solute Solubility in Dry Organic Solvents at 298 K

Three specific conditions must be met in order to use the Abraham solvation parameter model to predict saturation solubilities. First, the same solid phase must be in equilibrium with the saturation solutions in the organic solvent and in water (i.e., there should be no solvate or hydrate formation). Second, the secondary medium activity coefficient of the solid in the saturated solutions must be unity (or near unity). This condition generally restricts the method to those solutes that are sparingly soluble in water and nonaqueous solvents. Finally, for solutes that are ionized in aqueous solution, $C_{A,water}$, refers to the solubility of the neutral form. The second restriction may not be as important as initially believed. The Abraham solvation parameter model has shown remarkable success in correlating the solubility of several very soluble crystalline solutes. For example, Eqns 5 and 6 described the molar solubility of benzil in 24 organic solvents to within overall standard deviations of 0.124 and 0.109 log units, respectively. Standard deviations for acetylsalicylic acid dissolved in 13 alcohols, 4 ethers and ethyl acetate were 0.123 and 0.138 log units. Benzil (Acree and Abraham, 2002) and acetylsalicylic acid (Charlton *et al*., 2003) exhibited solubilities exceeding 1Molar in several of the organic solvents studied. In the case of acetylsalicylic acid it could be argued that the model's success relates back to when the equation coefficients were originally calculated for the dry solvents. The databases used in the regression analyses contained very few carboxylic acid solutes (benzoic acid, 2-hydroxybenzoic acid and 4-hydroxybenzoic acid). Most of the experimental data for carboxylic acids and other very acidic solutes was in the form of saturation solubilities, which were also in the 1 to 3 Molar range. Such arguments do not explain why equations (5) and (6) described the measured benzil solubility data. The benzil solubilities were measured after most of the equation coefficients were first determined.

4. High throughput experimental methods for measuring water-to-octanol partition coefficients

Each administered drug has to pass several membrane barriers in order to be delivered to the desired target site for therapeutic action. Orally administered drugs have to be absorbed into the intestine. Transdermally administered drugs need to penetrate human skin. Drugs intended to act in the central nervous system must cross the blood-brain brain barrier (BBB). This barrier is formed by the endothelial cells of the cerebral capillaries and restricts the transport of many compounds into the brain from the blood stream. The cellular architecture of the human intestine, human skin and human brain are quite different; however, the principle of transcellular absorption is the same. The dissolved drug must be transferred from an aqueous environment into the membrane phase, must diffuse across the membrane, and afterwards must partition back into an aqueous-phase compartment. The water-to-octanol partition coefficient, $P_{o/w}$, is widely regarded in the pharmaceutical industry as a quantitative measure for assessing a drug molecule's affinity for the membrane phase. Considerable attention has been afforded to developing high throughput experimental methodologies that either directly measure $P_{o/w}$ values, or that enable accurate estimation of $P_{o/w}$ from other conveniently measured properties. Poole and Poole (2003) reviewed the direct and indirect separation for obtaining water-to-octanol partition coefficients, with emphasis on the high throughput methods.

As selected examples of experimental methods that have been developed in recent years, Faller and coworkers (2005) designed a rather novel high throughput method to measure lipophilicity based on the diffusion of organic compounds between to aqueous phase

compartments separated by a thin 1-octanol liquid layer coated on a polycarbonate filter. The apparatus is shown in Figure 5. The molar concentration of the compound in the aqueous acceptor compartment, $C_{acceptor,end}$ is measured at the end of the defined time endpoint, tend. The apparent membrane permeability, P_{app}, is calculated from $C_{acceptor,end}$ by

$$P_{app} = -\left(\frac{V_{acceptor}\,V_{donor}}{V_{acceptor}+V_{donor}}\right)\left(\frac{1}{A\,t_{end}}\right)\ln\left(1-\frac{C_{acceptor,end}}{C_{equ}}\right) \tag{7}$$

$$C_{equ} = \left(\frac{V_{donor}}{V_{donor}+V_{acceptor}}\right) C_{donor,initial} \tag{8}$$

where $V_{acceptor}$ and V_{donor} denote the aqueous phase volumes in the acceptor and donor compartments, respectively, $C_{donor,initial}$ refers to the initial compound concentration in the donor phase, and A is the membrane accessible surface area times porosity. The water-to-octanol partition coefficient, $P_{o/w}$, is derived from the measured apparent permeability using a calibration curve constructed from measured permeabilities of standard compounds of known $P_{o/w}$ values. The assay has been used to measure water-to-hexadecane partition coefficients (Wohnsland and Faller, 2001) and can be performed using 96-well microtiter plates.

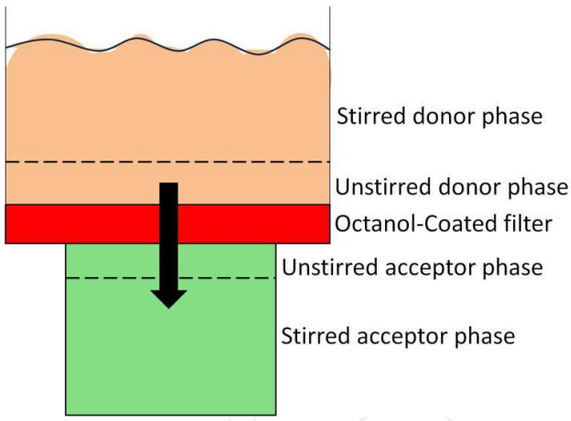

Fig. 5. High throughput experimental method for measuring water-to- octanol partition coefficients based on the diffusion of a solute betweentwo aqueous phase compartments.

Gao *et al*. (2005) developed a miniaturized method involving the dispersion of colloidal stable porous silica-encapsulated magnetic nanoparticles into water and/or an aqueous-buffered solution. Prior to dispersion, the nanoparticles are preloaded with a known amount of 1-octanol. Equilibrium is quickly established between the drug dissolved in the aqueous (or aqueous-buffered) solution and the small octanol droplets on the nanoparticles. The paramagnetic properties of the nanoparticles facilitate magnetic-induced phase separation. Once the magnetic particles are removed, the uv/visible absorbance of the solution is recorded. The log $P_{o/w}$ (or log Do/w in the case of an ionic solute) is calculated as

$$\log P_{o/w} = \log\left[\left(\frac{Abs_{before}-Abs_{after}}{Abs_{after}}\right)\left(\frac{V_{aqueous}}{V_{octanol}}\right)\right] \tag{9}$$

where Abs_{before} and Abs_{after} refer to the measured uv/visible absorbance of the aqueous solution prior and after partitioning, respectively, and $V_{aqueous}/V_{octanol}$ is the ratio of the aqueous phase volume divided by the volume of the octanol phase.

Henchoz and coworkers (2010) determined the water-to-octanol partition coefficients of 21 acidic and 29 basic pharmaceutical compounds using microemulsion electrokinetic capillary chromatography (MEEKC) coupled with uv absorption and mass spectrometric detection. The method involves measuring the retention factor of the investigated compound

$$k_{solute} = \frac{(t_{r,solute} - t_{r,eof})}{(1 - \frac{t_{r,solute}}{t_{r,mc}})t_{r,eof}} \quad (10)$$

where $t_{r,solute}$, $t_{r,eof}$ and $t_{r,mc}$ are the retention/migration times of the investigated drug compound, a highly hydrophilic neutral marker (such as dimethyl sulfoxide) and a highly lipophilic pseudostationary phase marker (such as dodecanophenone or 1-phenyldodecane). The migration times of the two markers define the migration window. The log $P_{o/w}$ of the drug molecules are obtained from a calibration curve

$$\log k_{solute} = \text{slope} \cdot \log P_{o/w} + \text{intercept} \quad (11)$$

established with the measured retention factors of standard compounds with known log $P_{o/w}$ values. The proposed method was validated using a set of 35 well-balanced reference compounds that contained neutral, acidic ($pK_a > 3.6$) or basic ($pK_a < 5.5$) compounds with log $P_{o/w}$ values ranging from 0.7 to 4.8. The acidic compounds were analyzed at a pH = 2, while the neutral and basic compounds were analyzed at pH = 10. The authors found that the log $P_{o/w}$ values based on MEEKC method differed by less than 0.5 log units from the log $P_{o/w}$ values determined by the more traditional shake-flask method. The method allowed log $P_{o/w}$ measurement in less than 20 minutes, which is acceptable for quick screening methods. The authors further noted that the MEEKC method could be easily automated, consumed very little sample and solvent, and did not require a highly purified drug sample.

Logarithms of the water-to-organic solvent partition coefficients represent another solute property that has been successfully correlated by Eqn. 12 of the Abraham solvation parameter model.

$$\text{Log P} = c + e \cdot \mathbf{E} + s \cdot \mathbf{S} + a \cdot \mathbf{A} + b \cdot \mathbf{B} + v \cdot \mathbf{V} \quad (12)$$

In Table 3 we have compiled the equation coefficients that have been reported describing the various water-to-organic solvent partitioning systems that have been studied. In the case of the alkane and chloroalkane (dichloromethane, trichloromethane, tetrachloromethane, 1,2-dichloroethane and 1-chlorobutane) solvents, one will note that the equation coefficients for describing log P are identical to the coefficients for correlating the log molar solubility ratios, log ($C_{A,organic}/C_{A,water}$) values. As noted previous the molar solubility ratios describe a "hypothetic partitioning" processes for solute transfer to an anhydrous "dry" organic solvent. Solubility ratios and practical partition coefficients are nearly identical for solvents that are almost "completely" immiscible with water.

Water-organic solvent based biphasic systems are widely used in liquid-liquid extraction and in calculating Abraham model solute descriptors in accordance with Eqn. 12. For compounds that react with water, or for compounds that have very low aqueous solubilities, water-based

Wet Solvent	c	e	s	a	b	v
Butan-1-ol[a]	0.376	0.434	-0.718	-0.097	-2.350	2.682
Pentan-1-ol[a]	0.185	0.367	-0.732	0.105	-3.100	3.395
Hexan-1-ol[a]	-0.006	0.460	-0.940	0.142	-3.284	3.792
Heptan-1-ol[a]	0.041	0.497	-0.976	0.030	-3.438	3.859
Octan-1-ol[a]	0.088	0.562	-1.054	0.034	-3.460	3.814
Nonan-1-ol[a]	-0.041	0.562	-1.103	0.090	-3.540	3.922
Decan-1-ol[a]	-0.136	0.542	-0.989	0.046	-3.722	3.996
Isobutanol[a]	0.249	0.480	-0.639	-0.050	-2.284	2.758
Olely alcohol [a]	-0.096	0.148	-0.841	-0.438	-4.040	4.125
Dichloromethane	0.319	0.102	-0.187	-3.058	-4.090	4.324
Trichloromethane	0.191	0.105	-0.403	-3.112	-3.514	4.395
Tetrachloromethane	0.199	0.523	-1.159	-3.560	-4.594	4.618
1,2-Dichloroethane	0.183	0.294	-0.134	-2.801	-4.291	4.180
1-Chlorobutane	0.222	0.273	-0.569	-2.918	-4.883	4.456
Butane	0.297	-0.005	-1.584	-3.188	-4.567	4.562
Pentane	0.369	0.386	-1.568	-3.535	-5.215	4.514
Hexane	0.361	0.579	-1.723	-3.599	-4.764	4.344
Heptane	0.325	0.670	-2.061	-3.317	-4.733	4.543
Octane	0.223	0.642	-1.647	-3.480	-5.067	4.526
Nonane	0.240	0.619	-1.713	-3.532	-4.921	4.482
Decane	0.160	0.585	-1.734	-3.435	-5.078	4.582
Undecane	0.058	0.603	-1.661	-3.421	-5.120	4.619
Dodecane	0.114	0.668	-1.664	-3.545	-5.006	4.459
Hexadecane	0.087	0.667	-1.617	-3.587	-4.869	4.433
Cyclohexane	0.159	0.784	-1.678	-3.740	-4.929	4.577
Methylcyclohexane	0.246	0.782	-1.982	-3.517	-4.293	4.528
Isooctane	0.318	0.555	-1.737	-3.677	-4.864	4.417
Benzene	0.142	0.464	-0.588	-3.099	-4.625	4.491
Toluene	0.143	0.527	-0.720	-3.010	-4.824	4.545
Fluorobenzene	0.139	0.152	-0.374	-3.030	-4.601	4.540
Chlorobenzene	0.065	0.381	-0.521	-3.183	-4.700	4.614
Bromobenzene	-0.017	0.436	-0.424	-3.174	-4.558	4.445
Iodobenzene	-0.192	0.298	-0.308	-3.213	-4.653	4.588
Nitrobenzene	-0.152	0.525	0.081	-2.332	-4.494	4.187
Diethyl ether[a]	0.248	0.561	-1.016	-0.226	-4.553	4.075
Diisopropyl ether[a]	0.472	0.413	-0.745	-0.632	-5.251	4.059
Dibutyl ether	0.252	0.677	-1.506	-0.807	-5.249	4.815
o-Nitrophenyl octyl ether	0.121	0.600	-0.459	-2.246	-3.879	3.574
Ethyl acetate[a]	0.441	0.591	-0.699	-0.325	-4.261	3.666
Butyl acetate[a]	-0.475	0.428	-0.094	-0.241	-4.151	4.046
PGDP[b]	0.256	0.501	-0.828	-1.022	-4.640	4.033
Methyl isobutyl ketone	0.383	0.801	-0.831	-0.121	-4.441	3.876
Olive oil	-0.035	0.574	-0.798	-1.422	-4.984	4.210

Carbon disulfide	0.047	0.686	-0.943	-3.603	-5.818	4.921
Isopropyl myristate	-0.605	0.930	-1.153	-1.682	-4.093	4.249
Triolein	0.385	0.983	-2.083	-2.007	-3.452	4.072

[a] Correlation uses the Bo solute descriptor.
[b] Propylene glycol dipelargonate.

Table 3. Coefficients in Eqn. 12 for Correlating Solute Water-to-Organic Solvent log P values at 298 K

Wet Solvent	c	e	s	a	b	l
Butan-1-ol	-0.095	0.262	1.396	3.405	2.565	0.523
Pentan-1-ol	-0.107	-0.001	1.188	3.614	1.671	0.721
Hexan-1-ol	-0.302	-0.046	0.880	3.609	1.785	0.824
Heptan-1-ol	-0.159	0.018	0.825	3.539	1.425	0.830
Octan-1-ol	-0.198	0.002	0.709	3.519	1.429	0.858
Nonan-1-ol	-0.197	0.141	0.694	3.616	1.299	0.827
Decan-1-ol	-0.302	0.233	0.741	3.531	1.177	0.835
Isobutanol	-0.095	0.262	1.396	3.405	2.565	0.523
Olely alcohol	-0.268	-0.392	0.800	3.117	0.978	0.918
Dichloromethane	0.192	-0.572	1.492	0.460	0.847	0.965
Trichloromethane	0.157	-0.560	1.259	0.374	1.333	0.976
Tetrachloromethane	0.217	-0.435	0.554	0.000	0.000	1.069
1,2-Dichloroethane	0.017	-0.337	1.600	0.774	0.637	0.921
1-Chlorobutane	0.130	-0.581	1.114	0.724	0.000	1.016
Butane	0.291	-0.360	0.091	0.000	0.000	0.959
Pentane	0.335	-0.276	0.000	0.000	0.000	0.968
Hexane	0.292	-0.169	0.000	0.000	0.000	0.979
Heptane	0.275	-0.162	0.000	0.000	0.000	0.983
Octane	0.215	-0.049	0.000	0.000	0.000	0.967
Nonane	0.200	-0.145	0.000	0.000	0.000	0.980
Decane	0.156	-0.143	0.000	0.000	0.000	0.989
Undecane	0.113	0.000	0.000	0.000	0.000	0.971
Dodecane	0.017	0.000	0.000	0.000	0.000	0.989
Hexadecane	0.000	0.000	0.000	0.000	0.000	1.000
Cyclohexane	0.163	-0.110	0.000	0.000	0.000	1.013
Methylcyclohexane	0.318	-0.215	0.000	0.000	0.000	1.012
Isooctane	0.264	-0.230	0.000	0.000	0.000	0.975
Benzene	0.107	-0.313	1.053	0.457	0.169	1.020
Toluene	0.121	-0.222	0.938	0.467	0.099	1.012
Fluorobenzene	0.181	-0.621	1.432	0.647	0.000	0.986
Chlorobenzene	0.064	-0.399	1.151	0.313	0.171	1.032
Bromobenzene	-0.064	-0.326	1.261	0.323	0.292	1.002
Iodobenzene	-0.171	-0.192	1.197	0.245	0.245	1.002
Nitrobenzene	-0.296	0.092	1.707	1.147	0.443	0.912
Benzonitrile	-0.067	-0.257	1.848	2.009	0.227	0.870

Diethyl ether	0.206	-0.169	0.873	3.402	0.000	0.882
Dipropyl ether	0.065	-0.202	0.776	3.074	0.000	0.948
Diisopropyl ether	0.114	-0.032	0.685	3.108	0.000	0.941
Dibutyl ether	0.369	-0.216	0.026	2.626	-0.499	1.124
Ethyl acetate	0.130	0.031	1.202	3.199	0.463	0.828
Butyl acetate	-0.664	0.061	1.671	3.373	0.824	0.832
Methyl isobutyl ketone	0.244	0.183	0.987	3.418	0.323	0.854
Olive oil	-0.156	-0.254	0.859	1.656	0.000	0.873
Carbon disulfide	0.101	0.251	0.177	0.027	0.095	1.068
Triolein	0.147	0.254	-0.246	1.520	1.473	0.918

Table 4. Coefficients in Eqn. 2 for Correlating Solute Gas-to-Organic Solvent log K values at 298 K

partitioning systems may not be appropriate. Poole and coworkers (Karunasekara and Poole, 2010; Qian and Poole, 2007; Ahmed and Poole, 2006a,b) have reported Abraham model correlations for several totally organic biphasic systems, such as heptane + formamide, hexane + acetonitrile, heptane + methanol, heptane + N,N-dimethylformamide, heptane + 2,2,2-trifluoroethanol, and heptane + 1,1,1,3,3,3-hexafluoroisopropanol. The organic-based biphasic systems allow one to calculate solute descriptors for compounds that might not otherwise be possible with water-based partitioning systems. For example, the biphasic hexane + acetonitrile, heptane + N,N-dimethylformamide, and heptane + 2,2,2-trifluoroethanol systems were used, in combination with chromatographic retention factors, to determine a complete set of descriptors for organosilicon compounds (Atapattu and Poole, 2009; Ahmed *et al*., 2007), many of which react with water. Abraham model equation coefficients are tabulated in Table 5 for seven organic solvent-to-organic solvent partitioning systems.

Partitioning system	c	e	s	a	b	v
Formamide-to-heptane	0.083	0.559	-2.244	-3.250	-1.614	2.384
N,N-Dimethylformamide-to-heptane	0.065	0.030	-1.405	-2.039	-0.806	0.721
2,2,2-Trifluoroethanol-to-heptane	0.160	0.856	-1.538	-1.325	-2.965	1.190
1,1,1,3,3,3-Hexafluoroisopropanol-to-heptane	-0.225	0.720	-1.357	-0.577	-2.819	1.161
Methanol-to-heptane	-0.056	0.164	-0.620	-1.337	-0.957	0.507
Ethylene glycol-to-heptane	0.343	0.000	-1.247	3.807	-2.194	2.065
Acetonitrile-to-hexane	0.097	0.189	-1.332	-1.649	-0.966	0.773

Table 5. Coefficients in Eqn. 12 for Correlating Solute Organic Solvent-to-Organic Solvent log P values at 298 K

5. Calculation of Abraham solute descriptors from measured solubility and partition coefficient data

The application of Eqn. 1 and Eqn. 2 requires a knowledge of the descriptors (or properties) of the solutes: **E**, **S**, **A**, **B**, **V** and **L**. The descriptors **E** and **V** are quite easily obtained. **V** can be calculated from atom and bond contributions as outlined previously (Abraham and McGowan, 1987). The atom contributions are in Table 6; note that they are in cm^3 mol^{-1}. The

bond contribution is 6.56 cm^3 mol^{-1} for each bond, no matter whether single, double, or triple, to be subtracted. For complicated molecules it is time consuming to count the number of bonds, Bn, but this can be calculated from the algorithm given by Abraham (1993a)

$$Bn = Nt - 1 + R \tag{13}$$

where Nt is the total number of atoms in the molecule and R is the number of rings.
Once **V** is available, **E** can be obtained from the compound refractive index at 20°C. If the compound is not liquid at room temperature or if the refractive index is not known the latter can be calculated using the freeware software of Advanced Chemistry Development (ACD). An Excel spreadsheet for the calculation of **V** and **E** from refractive index is available from the authors. Since **E** is almost an additive property, it can also be obtained by the summation of fragments, either by hand, or through a commercial software program (ADME Boxes, 2010). There remain the descriptors **S**, **A**, **B**, and **L** to be determined.
Partition coefficients and/or solubilities can be used to obtain all the four remaining descriptors (Abraham *et al*., 2004). Suppose there are available solubilities for a given compound in water and a number of solvents. Then solubility ratios, log ($C_{A,organic}/C_{A,water}$), can be obtained as shown in Eqn. 5 and Eqn. 6. If three solubility ratios are available for three solvent systems shown in Table 1, we have three equations and three unknowns (**S**, **A**, and **B**) so that the latter can be determined. Of more practical use is a situation where several solubility ratios are known. Then if we have, say, six solubility ratios and three equations, the three unknowns can be obtained as the descriptors that give the best fit to the six equations. The Solver add-on program to Excel can be set up to carry out such a calculation automatically. However, it is possible to increase the number of equations by the stratagem of converting the water-to-solvent solubility ratios into gas to solvent solubility ratios, $C_{A,organic}/C_{A,gas}$

$$C_{A,organic}/C_{A,water} * C_{A,water}/C_{A,gas} = C_{A,organic}/C_{A,gas} \tag{14}$$

The ratio $C_{A,water}/C_{A,gas}$ is the gas-to-water partition coefficient, usually denoted as K_w. A further set of equations is available for gas-to-solvent solubility ratios, Table 2. Thus six water-to-solvent solubility ratios can be converted into six gas-to-solvent solubility ratios, leading to a set of 12 equations. If $\log K_w$ is not known, it can be used as another parameter to be determined. This increases the number of unknowns from four (**S, A, B, L**) to five (**S, A, B, L**, $\log K_w$) but the number of equations is increased from six to twelve. In addition, two equations are available for gas to solvent partitions themselves, see the last entries in Tables 1 and 2, making for the present case no fewer than fourteen equations.
As an example, we use data on solubilities of trimethoprim in eight solvents (Li *et al*., 2008) converted from mol fraction to mol dm^{-3}. The solubility in water was not given, but is known to be $2.09 * 10^{-3}$ in mol dm^{-3} (Howard and Meylan, 1997). The eight observed solubility ratios, $C_{A,organic}/C_{A,water}$, are in Table 7, as log (ratio). We took log K_w as another parameter to be determined, leading to no less than 18 equations: the eight original equations from solubilities in the eight solvents that led to $C_{A,organic}/C_{A,water}$, the corresponding eight equations for $C_{A,organic}/C_{A,gas}$, and two equations for $C_{A,water}/C_{A,gas}$ (*ie* K_w). With **E** fixed at 1.892 and **V** fixed at 2.1813, the best fit values of the descriptors were **S** = 2.52, **A** = 0.44, **B** = 1.69, **L** = 11.81 and log K_w = 14.49; these yielded the calculated log (ratios) in Table 7. For all 18 values, the Average Error = -0.002, the Absolute Average Error = 0.092, the RMSE = 0.107, and the SD = 0.110 log unit. Not only do the original solubilities allow the derivation of descriptors for trimethoprim, but the latter, in turn, allow the prediction of solubility ratios and hence actual solubilities in all the solvents listed in Table 1.

Exactly the same procedure is adopted if actual partition coefficients are experimentally available, rather than solubilities. The relevant equations are now those in Table 3 and Table 4. Of course if both solubilities and actual partition coefficients have both been experimentally determined, a combination of equations from Tables 1 and 2 and from Tables 3 and 4 can be used. Even though partition coefficients refer to partition into wet solvents, descriptors obtained from partition coefficients using equations in Table 3 and Table 4 can still be used to predict solubility ratios and solubilities in dry solvents for all the solvents listed in Table 1.

C	16.35		N	14.39		O	12.43
Si	26.83		P	24.87		S	22.91
Ge	31.02		As	29.42		Se	27.81
Sn	39.35		Sb	37.74		Te	36.14
Pb	43.44		Bi	42.19			
H	8.71		He	6.76		B	18.32
F	10.48		Ne	8.51		Hg	34.00
Cl	20.95		A	1.90			
Br	26.21		Kr	2.46			
I	34.53		Xe	3.29			
			Rn	3.84			

Table 6. Atom contributions to the McGowan volume, in cm^3 mol^{-1}

Water-to-solvent	calc	obs
Methanol	1.35	1.48
Ethanol	0.98	0.94
Propanol	0.75	0.80
Butanol	0.53	0.68
2-Propanol	0.61	0.51
2-Butanol	0.65	0.62
Tetrahydrofuran	1.18	1.02
Propanone	0.90	0.94
Gas to water	14.48	14.49
Gas-to-solvent	calc	obs
Methanol	15.81	15.97
Ethanol	15.48	15.43
Propanol	15.23	15.29
Butanol	15.02	15.18
2-Propanol	15.14	15.01
2-Butanol	15.18	15.11
Tetrahydrofuran	15.70	15.51
Propanone	15.34	15.43
Gas to water	14.53	14.49

Table 7. Solubility ratios for trimethoprim, as log (ratio)

Although we have set out the determination of descriptors from experimental measurements, it is still very helpful to use the ACD software (ADME Boxes, 2010) to calculate the descriptors at the same time. Occasionally there may be erroneous solubility measurements, or solubilities may be affected through solvate formation, and the calculated descriptors afford a useful check on the obtained descriptors from experiment measurements.

6. Abraham solvation parameter model: prediction of blood-to-brain and blood-to-iissue partition coefficient

Successful drug development requires efficient delivery of the drug to the target site. The drug must cross various cellular barriers by passive and/or transporter-mediated uptake. Drug delivery to the brain is particularly challenging as there are two physiologically barriers – the blood-brain barrier (BBB) and the blood-cerebrospinal fluid barrier (BCSFB) – separating the brain from its blood supply controlling the transport of chemical compounds. The BBB is a continuous layer of microvessel endothelial cells, connected by highly-developed tight junctions, which effectively restrict paracellular transport of molecules irrespective of their molecular size. Tight junctions provide significant transendothelial electrical resistance to the brain microvessel endothelial cells and serves to further impede the penetration of the BBB. The electrical resistance between the endothelial cells is on the order of 1500 – 2000 Ω/cm^2, as compared to and electrical resistance of 3.33 Ω/cm^2 found in other body tissues (Alam *et al*., 2010). Under normal conditions the BBB acts as a barrier to toxic agents and safeguards the integrity of the brain. A compound may circumvent the BBB and gain access to the brain by the nose-to-brain route. The compound is transported to the brain via an olfactory pathway following absorption across the nasal mucosa.

Alternatively, compounds may permeate from the blood into the cerebrospinal fluid and permeate into the brain interstitial fluid. The BCSFB separates the blood from the cerebrospinal fluid (CSF) that runs in the subarachnoid space surrounding the brain. The BCSFB is located at the choroid plexus, and it is composed of epithelial cells held together at their apices by tight junctions, which limit paracellular flux. Hence compounds penetrate the barrier transcellularly. The CSF-facing surface of the epithelial cells, which secrete CSF into the ventricles, is increased by the presence of microvilli. The capillaries in the choroid plexus allow free movement of molecules via fenestractions and intracellular gaps. Transport across the BCSFB is not an accurate measure of transport across the BBB as the two barriers are anatomically different. However, as Begley *et al.* (2000) point out, for many compounds there is a permanently maintained concentration gradient between brain interstitial fluid and the CSF.

The transport of compounds into the brain can take place through 'passive' transport or 'active' transport. Nearly all the calculational models for transport into the brain deal with passive transport, although it is now known that many compounds are prevented from crossing the BBB through efflux mechanisms especially involving P-glycoprotein. The use of wildtype mice and knockout mice (the latter deficient in Pgp) has shown conclusively that for a number of drugs the brain to plasma distribution is much lower for the wildtype mice than for knockout mice. We will focus on passive transport, but it must be appreciated that any analysis might well include compounds that are actually subject to active transport and will appear as outliers in the analyses.

The steady-state distribution of a compound between the blood (or plasma) and brain, and the rate of permeation of a compound from blood (or from an aqueous saline solution) through the blood brain barrier, are two quantitative measures of drug uptake in the brain.

The logarithm of the blood-to-brain concentration ratio, log BB, is a thermodynamic quantity defining the extent of blood penetration. The log BB is mathematically given by

$$\log BB = (\frac{C_{solute,brain}}{C_{solute,blood}}) \tag{15}$$

the ratio of the solute concentration in brain tissue divided by the solute's concentration in blood (or serum or plasma) at steady-state conditions. The blood/brain distribution ratio can be experimentally determined by intravenous administration of a single injection of ^{14}C-radioactive isotope labeled test substance in rats. The animal is sacrificed at a specified time endpoint after equilibrium is achieved. The brain and blood are immediately harvested, and the concentration in each biological sample is quantified from the measured radioactivity. Isotopic labeling provides a convenient means to distinguish the injected test substance from all other chemicals that might be present in the body. Radioactive counting methods do not distinguish between the radioactive isotope in the injected test substance and any degradation products that might have been formed before the animal was sacrificed. The distribution experiments are usually carried out over a long time scale, possibly hours, and concentrations in blood and brain obtained as a function of time. The ratio, as Eq. 15, will change with time and only if it reaches a constant value can the ratio be taken as an equilibrium value. This is very time consuming indeed, as only one measurement can be made with each rat. Despite these shortcomings, radioactive labeling is one of the more popular methods for not only determining the blood-to-brain distribution coefficient, but other blood-to-tissue partition coefficients as well.

Blood-to-brain and blood-to-tissue partition coefficients have also been measured for volatile organic compounds using the *in vitro* vial method (see Figure 6). A known amount of animal sample is placed in a glass vial of known volume. The vial is then sealed and a minute known quantity of the volatile organic compound (VOC) is introduced by syringe through the rubber septum. After equilibration a sample of the headspace vapor phase is withdrawn from the glass vial for gas chromatographic analysis. The gas-to-tissue partition coefficient is computed from mass balance considerations as the total amount of solute added, the concentration of the vapor phase, the headspace volume and amount of tissue sample are all known. The blood-to-tissue partition coefficient, $P_{tissue/blood}$, is calculated as

$$P_{tissue/blood} = P_{tissue/air} x P_{air/blood} = (\frac{C_{solute,tissue}}{C_{solute,air}}) x (\frac{C_{solute,air}}{C_{solute,blood}}) \tag{16}$$

the product of the measured air-to-tissue partition coefficient, $P_{tissue/air}$, times the measured blood-to-air partition coefficient, $P_{air/blood}$. The *in vitro* partition coefficient data are important and are used as required input parameters in pharmacokinetic models developed to determine the disposition of volatile organic compounds that individuals inhale in the workplace and in the environment.

Abraham and coworkers (2006a) reported correlation models for the air-to-brain ($P_{brain/air}$) and blood-to-brain ($P_{brain/blood}$) partition coefficients for VOCs in humans and rats

$$\begin{aligned} \text{Log } P_{brain/air}\,(\textit{in vitro}) &= -0.987 + 0.263\mathbf{E} + 0.411\mathbf{S} + 3.358\mathbf{A} + 2.025\mathbf{B} + 0.591\mathbf{L} \\ &\left(N = 81,\ R^2 = 0.923,\ SD = 0.346,\ RMSE = 0.333,\ F = 179.0\right) \end{aligned} \tag{17}$$

$$\text{Log BB} = \text{Log P}_{\text{brain/blood}}(\textit{in vitro}) = -0.057 + 0.017\mathbf{E} - 0.536\mathbf{S} - 0.323\mathbf{A} - 0.335\mathbf{B} + 0.731\mathbf{V}$$
$$(\text{N} = 78,\ \text{R}^2 = 0.725,\ \text{SD} = 0.203,\ \text{RMSE} = 0.196,\ \text{F} = 37.9) \quad (18)$$

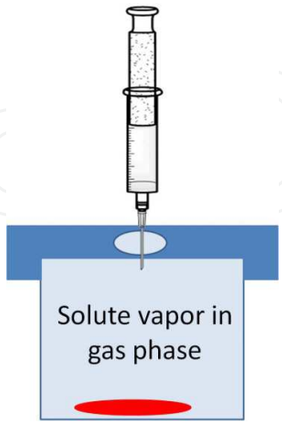

Fig. 6. Equilibrium vial technique depicting removal of the equilibrated headspace vapor above the animal/human tissue

In Eqns. 17 and 18, N is the number of data points in the regression analysis, R^2 represents the squared correlation coefficient, SD denotes the standard deviation and RMSE corresponds to the root mean square error. Note that in a multiple linear regression equation, the denominator in the definition of SD is N – P – 1 and in the definition of RMSE it is N – P, where P is the number of independent variables in the equation. The derived correlations provided a reasonably accurate mathematical description of the observed partition coefficient data as evidenced by the high squared correlation coefficients and reasonably small standard deviations. Both correlations were validated using training set and test set analyses. In comparing calculated biological data to observed values one must remember that the measured values do have larger experimental uncertainties. A reasonable estimated uncertainty for the measured log $P_{brain/air}$ would be about 0.2 log units based on independent values from different laboratories. Rat and human partition coefficient data for each given VOC were averaged (if both values were available), and the average values were combined into a single regression analysis. In a comparison of experimental human and rat partition coefficient data for 17 common compounds, the authors had shown that the two sets of data (human versus rat) differed by only 0.062 log units, which is likely less than the experimental uncertainty associated with the measured experimental values. For the compounds studied, human and rat partition coefficient data were identical for all practical purposes. The authors also showed that blood-to-brain and plasma-to-brain partition coefficients were sufficiently close and could be combined into a single Abraham model correlation

$$\log \text{P}_{\text{brain/(blood,plasma)}} = -0.028 + 0.003\,\mathbf{E} - 0.485\,\mathbf{S} - 0.117\,\mathbf{A} - 0.408\,\mathbf{B} + 0.703\,\mathbf{V}$$
$$(\text{N} = 99,\ \text{R}^2 = 0.703,\ \text{SD} = 0.197,\ \text{RMSE} = 0.191,\ \text{F} = 44.1) \quad (19)$$

Eqs. (18) and (19), are not substantially different, and the statistics are almost the same. It is a moot point as to whether further values of blood to brain partition coefficients should best be predicted through Eqn. 18 or 19. We recommend that Eqn. 18 be used to predict blood-to-

brain partition coefficients of VOC because it refers specifically to blood rather than to blood or plasma.

A follow-up study (Abraham *et al*., 2006b) considered the partitioning behavior of drugs and drug candidates (measured by *in vivo* experimental methods), as well as the VOC *in vitro* partition coefficient data discussed above. The Abraham model correlation for the *in vivo* log $P_{brain/blood}$ data

$$\log BB = \log P_{brain/blood}(in\ vivo) = 0.547 + 0.221\mathbf{E} - 0.604\mathbf{S} - 0.641\mathbf{A} - 0.681\mathbf{B} + 0.635\mathbf{V} - 1.216\mathbf{Ic}$$
$$(N = 233,\ R^2 = 0.75,\ SD = 0.33,\ F = 113) \tag{20}$$

differs from the correlation equation for the VOCs (see Eqn. 18). In particular, the c-coefficients differ appreciably 0.547 (SD = 0.078) as against -0.024 (SD=0.069), which suggests that there is a systematic difference between the *in vivo* and *in vitro* distributions. The authors went on to show that the difference resulted in part because the two sets of compounds (drugs versus VOCs) inhabit different areas in chemical space. The *in vivo* drug compounds had much larger solute descriptors, and included compounds having a carboxylic acid functional group. The independent variable **Ic** was needed as an indicator descriptor for carboxylic acids (**Ic** = 1 for carboxylic acids, **Ic** = 0 for noncarboxylic acid solutes).

The blood-to-brain partition coefficient provides valuable information regarding a compound's ability to penetrate the blood-brain barrier. Cruciani *et al*. (2000) noted that compounds having log BB values greater than 0.0 (concentration in the brain exceeds concentration in the blood) should cross the barrier, whereas compounds having log BB less than -0.3 tended not to cross the barrier. Li and coworkers (2005) used a slightly different classification scheme (see Figure 7) of dividing compounds into BBB-penetrating (BBB+) or BBB-non-penetrating (BBB-) according to whether the log BB value was ≥ -1 or ≤ -1, respectively. Many times an actual numerical log BB is not needed in the decision making process, and in such cases, an indication of BBB+ or BBB- is often sufficient. Zhao *et al*. (2007) proposed a fairly simple decision tree for classifying drug candidates as BBB+ or BBB- based on their Abraham solute descriptors (See Figure 7). Solute acidity and solute basicity were the two most important properties governing BBB penetration, with solute excess molar refraction playing a much smaller role. The proposed classification scheme correctly predicted the BBB penetration of 90 % of the 1093 compounds considered.

As noted above permeation of a compound from blood (or from an aqueous saline solution) through the blood brain barrier can be used to indicate drug uptake in the brain. The membrane permeability-surface area product, PS, is a kinetic parameter used in describing initial rate of unidirectional transfer

$$k_{in} = F(1 - e^{-PS/F}) \tag{21}$$

where k_{in} is the measured transfer constant and F is the perfusion fluid flow expressed in milliliters per second per gram. For solutes that bind rapidly and reversibly to plasma proteins, Eqn. 21 is modified as follows

$$k_{in} = F(1 - e^{-fu\,PS/F}) \tag{22}$$

assuming that the unbound and bound forms of the drug are in equilibrium in the fluid. In Eqn. 22, fu is the fraction of the unbound drug in the perfusion fluid. In a typical experiment,

the drug (dissolved in blood or in an aqueous saline solution) is perfused into the internal carotid artery and the rate of drug uptake is determined by a radioisotope assay method. The animals are sacrificed at various time intervals. The time scale needed to perform the perfusion study is very short – typically no more than a few minutes. Because of the small time scale, perfusion measurements are less subject to degradation effects than are log BB measurements, although the same difficulties over passive and active transport still exist.

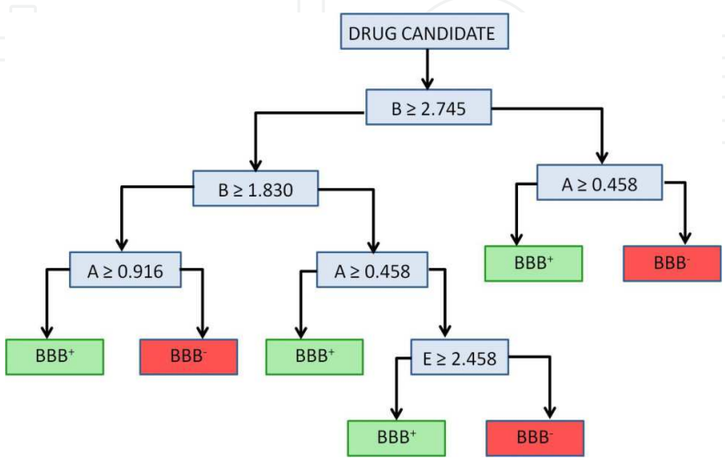

Fig. 7. Decision tree for predicting whether drugs pass through the BBB based on their Abraham solute descriptors. BBB+ indicates BBB penetrating whereas BBB- denotes BBB non-penetration. The right-handside of any decision branch is no penetration (red box), and the left-handside is yes penetration (green box). (The right-hand side of any decision branch is yes, and the left-hand side is no.)

Abraham (2004) derived the following mathematical correlation

$$\begin{aligned} &\log PS = -0.716 - 0.974\mathbf{S} - 1.802\mathbf{A} - 1.603\mathbf{B} + 1.893\mathbf{V} \\ &\left(N = 30,\ R^2 = 0.868,\ SD = 0.52,\ F = 42\right) \end{aligned} \tag{23}$$

by regression analysis of the experimental log PS data for 30 neutral compounds from protein-free saline solution buffered at pH of 7.4. The contribution of the $e \cdot \mathbf{E}$ term was not significant and was removed from Eqn. 23. The negative equation coefficients in Eqn. 23 indicate that an increase in compound polarity of any kind, that is dipolarity/polarizability, hydrogen-bonding acidity or hydrogen-bonding basicity, results in a decrease in the rate of permeation. Increased solute size (**V** solute descriptor), on the other hand, results in a greater permeation rate.

The Abraham model correlations that have been presented thus far pertain to neutral molecules. The basic model has been extended to include processes between condensed phases involving ions and ionic species

$$SP = c + e \cdot \mathbf{E} + s \cdot \mathbf{S} + a \cdot \mathbf{A} + b \cdot \mathbf{B} + v \cdot \mathbf{V} + j_+ \cdot \mathbf{J}^+ + j_- \cdot \mathbf{J}^- \tag{24}$$

by adding one new term for cations and one new term for anions. $\mathbf{J}^+$ is used whenever a cation is the solute, $\mathbf{J}^-$ whenever an anion is the solute, and neither is used whenever the solute is a nonelectrolyte. It is very important to note that the two new ionic descriptors

are used together with the descriptors originally chosen for nonelectrolytes. This ensures that values of **S**, **A** and **B** for ions and ionic species are on the same scale as those for nonelectrolytes. Solute descriptors have been reported for many simple cations and anions, for carboxylates, for phenoxides, and for protonated amines and protonated pyridines. The j_+ and j_- equation coefficients have been determined (Abraham and Acree, 2010a,b,c,d) for several of the organic solvents listed in Table 1. Abraham (2011) recently reanalyzed the published log PS data in terms of Eqn. 24 to yield the following correlation model

$$\log PS = -1.268 - 0.047\mathbf{E} - 0.876\mathbf{S} - 0.719\mathbf{A} - 1.571\mathbf{B} + 1.767\mathbf{V} + 0.469\mathbf{J}^{+} + 1.663\mathbf{J}^{-} \quad (25)$$
$$(N = 88,\ R^2 = 0.810,\ SD = 0.534,\ F = 48.8)$$

The 88 log PS values in Eqn. 25 were for compounds that existed in the saline perfusate entirely (or almost entirely) as neutral molecules or entirely (or almost entirely) as charged species, and which underwent perfusion by a passive process. Abraham showed that log PS values for carboxylate anions are about two log units less than those for the neutral carboxylic acids, and that log PS values for protonated base cations are about one log unit less than those for the neutral bases.

7. Abraham solvation parameter model: prediction of blood-to-tissue and gas-to-tissue partition coefficients

Air-to-blood partitioning is a major determinant governing the uptake of chemical vapors into the blood and their subsequent elimination from blood to exhaled air. Air partitioning processes are becoming increasing more important in the pharmaceutical industry given the large numbers of drugs and vaccines that are now administered by inhalation aerosols and nasal delivery devices. Inhalation drug delivery is appealing given the large surface area for drug absorption, the high blood flow to and from the lung, and the absence of first pass metabolism that is characteristic of the lung. Inhalation drug delivery results in both a rapid clearance action and a rapid onset of therapeutic action, and a reduction in the number of undesired side effects. Eixarch and coworkers (2010) proposed the development of a pulmonary biopharmaceutical classification system (pBCS) that would classify drugs according to their ability to reside in the lung or to be transferred to the bloodstream. The classification scheme would need to consider factors associated with the lung's biology (metabolism, efflux transporters, clearance) and with the drug formulation/physicochemical properties (solubility, lipophilicity, protein binding, particle size, aerosol physics). Blood-to-tissue partitionings govern the distribution throughout the rest of the body once the drug has entered the bloodstream.

Abraham model correlations have been developed to describe the air-to-tissue and blood-to-tissue partition coefficients of drugs and volatile organic compounds (VOCs). The derived mathematical equations include:

*Muscle (*Abraham *et al.,* 2006c):

$$\log K_{muscle/air}(\textit{in vitro}) = -1.039 + 0.207\mathbf{E} + 0.723\mathbf{S} + 3.242\mathbf{A} + 2.469\mathbf{B} + 0.463\mathbf{L} \quad (26)$$
$$(N = 114,\ R^2 = 0.944,\ SD = 0.267,\ F = 363)$$

$$\log P_{muscle/blood}(in\ vitro) = -0.185 - 0.209\mathbf{E} - 0.593\mathbf{S} - 0.081\mathbf{A} - 0.168\mathbf{B} + 0.741\mathbf{V} \quad (N = 110,\ R^2 = 0.537,\ SD = 0.207,\ F = 24) \tag{27}$$

$$\log P_{muscle/blood}(in\ vivo)\ 0.082 - 0.059\mathbf{E} + 0.010\mathbf{S} - 0.248\mathbf{A} + 0.028\ B + 0.110\mathbf{V} - 1.022\mathbf{Ic} \quad (N = 60,\ R^2 = 0.745,\ SD = 0.253,\ F = 25.9) \tag{28}$$

Fat (Abraham and Ibrahim, 2006):

$$\log K_{fat/air}(in\ vitro) = -0.052 + 0.051\mathbf{E} + 0.728\mathbf{S} + 1.783\mathbf{A} + 0.332\mathbf{B} + 0.743\mathbf{L} \quad (N = 129,\ R^2 = 0.958,\ SD = 0.194,\ F = 562.8) \tag{29}$$

$$\log P_{fat/blood}(in\ vitro) = 0.474 + 0.016\mathbf{E} - 0.005\mathbf{S} - 1.577\mathbf{A} - 2.246\mathbf{B} + 1.560\mathbf{V} \quad (N = 126,\ R^2 = 0.847,\ SD = 0.304,\ F = 132.7) \tag{30}$$

$$\log P_{fat/blood}(in\ vivo) = 0.077 + 0.249\mathbf{E} - 0.215\ \mathbf{S} - 0.902\mathbf{A} - 1.523\mathbf{B} + 1.234\mathbf{V} - 1.013\mathbf{Ic} \quad (N = 50,\ R^2 = 0.811,\ SD = 0.33\ F = 30.7) \tag{31}$$

Liver (Abraham *et al*., 2007a):

$$\log K_{liver/air}(in\ vitro) = -0.943 + 0.836\mathbf{S} + 2.836\mathbf{A} + 2.081\mathbf{B} + 0.561\mathbf{L} \quad (N = 124,\ R^2 = 0.927,\ SD = 0.256,\ F = 376.8) \tag{32}$$

$$\log P_{liver/blood}(in\ vitro) = -0.095 - 0.366\mathbf{S} - 0.357\mathbf{A} - 0.180\mathbf{B} + 0.730\mathbf{V} \quad (N = 125,\ R^2 = 0.583,\ SD = 0.228,\ F = 41.9) \tag{33}$$

$$\log P_{liver/blood}(in\ vivo) = 0.292 - 0.296\mathbf{S} - 0.334\mathbf{A} + 0.181\mathbf{B} + 0.337\mathbf{V} - 0.597\mathbf{Ic} \quad (N = 85,\ R^2 = 0.522,\ SD = 0.420,\ F = 17.3) \tag{34}$$

Lung (Abraham *et al*., 2008a):

$$\log K_{lung/air}(in\ vitro) = -1.250 + 0.639\mathbf{E} + 1.038\mathbf{S} + 3.661\mathbf{A} + 3.041\mathbf{B} + 0.420\mathbf{L} \quad (N = 44,\ R^2 = 0.968,\ SD = 0.250,\ F = 231.8) \tag{35}$$

$$\log P_{lung/blood}(in\ vitro) = -0.143 - 0.383\mathbf{B} + 0.308\mathbf{V} \quad (N = 43,\ R^2 = 0.264,\ SD = 0.190,\ F = 7.2) \tag{36}$$

Correlations obtained by regression analysis of experimental drug partition coefficient data are denoted as "*in vivo*", and correlations pertaining to volatile organic compound partitioning are indicated as "*in vitro*". Human and rat partition coefficient data were combined into data set used in the regression analyses. The independent variable **Ic** was

needed as an indicator descriptor for carboxylic acids (**Ic** = 1 for carboxylic acids, **Ic** = 0 for noncarboxylic acid solutes) for the *in vivo* correlations involving drug molecules. The *in vivo* data sets included partition coefficient data for drug molecules such as nalidixic acid and valproic acid. No carboxylic acid solutes were contained in the *in vitro* data sets. The poor R^2 statistics noted in several of the blood-to-tissue correlations are due, at least in part, to the small spread in the log P values and the increased experimental uncertainties as noted below. Each derived correlation was validated by training set and test set analyses. Based on the validation computations the derived correlations are expected to predict the log $K_{tissue/air}$ and log $P_{tissue/blood}$ values of additional compounds to within about 0.2 to 0.3 log units.

As an informational note, the experimental data sets for the *in vitro* Abraham model correlations were determined using the equilibrium vial method. The gas-to-tissue partition coefficient of the VOC was calculated from the measured vapor phase composition in the headspace above the given tissue. The measured *in vitro* gas-to-tissue partition coefficients were converted to the corresponding blood-to-tissue values, $P_{tissue/blood}$ values, through Eqn. 16. The $P_{tissue/blood}$ include the experimental uncertainty in both the $K_{tissue/air}$ and $P_{blood/air}$ values. Should the *in vitro* experimental air-to-blood partitioning data not be available for the conversion, one can estimate the needed $P_{blood/air}$ values from the three correlation models

$$\log K_{blood/air}(\text{human}) = -1.18 + 0.39\mathbf{E} + 0.97\mathbf{S} + 3.80\mathbf{A} + 2.69\mathbf{B} + 0.41\mathbf{L} \quad (N = 155,\ R^2 = 0.34,\ RSME = 0.332,\ F = 474) \tag{37}$$

$$\log K_{blood/air}(\text{rat}) = -0.75 + 0.56\mathbf{E} + 1.06\mathbf{S} + 3.64\mathbf{A} + 2.41\mathbf{B} + 0.29\mathbf{L} \quad (N = 127,\ R^2 = 0.91,\ SD = 0.29,\ RMSE = 0.286,\ F = 242) \tag{38}$$

$$\log K_{blood/air}(\text{human or rat}) = -1.069 + 0.456\mathbf{E} + 1.083\mathbf{S} + 3.738\mathbf{A} + 2.580\mathbf{B} + 0.376\mathbf{L} \quad (N = 196.\ R^2 = 0.938,\ SD = 0.324,\ RMSE = 0.319,\ F = 572.8) \tag{39}$$

reported by Abraham and coworkers (2005). For any fully characterized system/process (those with calculated values for the equation coefficients) further values of SP (see Eqns. 1 and 2) can be estimated for solutes with known values for the solute descriptors. Solute descriptors can be obtained by regression analysis of measured drug solubilities in organic solvents and measured water-to-solvent and organic solvent-to-organic solvent partition coefficients as discussed above.

8. Abraham solvation parameter model: prediction of water-to-skin and blood-to-skin partition coefficients and skin permeability coefficients

Human skin is an important permeation barrier that controls the entry of chemicals into the body. The barrier properties of skin depend primarily on the outer skin cells, which are called the stratum corneum. The stratum corneum consists of multiple non-living layers of densely packed keratin-filled cells embedded in a lipid-rich extracellular matrix containing a mixture of ceramides, fatty acids, cholesterol and triglycerides (Monteiro-Riviere *et al*., 2001). The multiple layers are 7 – 16 micrometers in total thickness in most regions of the human body; however, in the palms of the hands and soles of the feet a much total layer thickness

of 400 – 600 micrometers is found (Holbrook and Odland, 1974) For a chemical to be absorbed into the body after dermal exposure, it must first dissolve in the stratum corneum and then diffuse through the remaining epidermis sub-layers and into the dermis layer, from where it will eventually enter the blood stream. Passive diffusion is the mechanism by which chemicals move through the stratum corneum. Passage through the remaining sub-layers of the skin is more rapid.

Penetration of a compound into the skin is controlled by the compound's chemical structure and physicochemical properties. Lipophilicity and hydrogen-bonding character play a major role in a compound's skin absorption profile. In general, substances possessing the greater lipophilicity are more readily absorbed by the skin than compounds with lesser lipophilicity. Dermal absorption generally increases with increasing water-to-octanol partition coefficient from log $P_{OtOH/water}$ = -1 to log $P_{OtOH/water}$ = 3.5. Highly lipophilic compounds (those with log $P_{OtOH/water}$ > 5) pass easily through the stratum corneum, but are generally too water-insoluble to pass through the remaining epidermis sub-layers to enter the blood stream. There has been increasing experimental evidence that ionized species can contribute to transdermal absorption (Netzlaff *et al*., 2006; Abraham and Martins, 2004; Michaels *et al*., 1975). When the penetrating compound can exist in both ionized and unionized forms, it is the unionized form that penetrates faster through the lipid regions. Some contribution of the ionized form to the overall permeability, however, is expected. The solubilizing vehicle and formulation ingredients can alter the skin penetration of a compound by affecting the barrier properties of the skin by a range of mechanisms including hydration, delipidization, fluidization and desmosome disruption in the stratum corneum, or by changing the partitioning of the compound into the stratum corneum.

Skin partitioning is important in the pharmaceutical industry as many medications are applied topically to the skin in ointments, in creams, in lotions and gels, and in skin patches. Once applied, the medication often needs to find its way into the blood system for delivery to the desired target site. Abraham and Martins (2004) developed a mathematical correlation between the water-to-skin partition coefficient, K_{sc}, and the Abraham solute descriptors

$$\begin{aligned} \text{Log } K_{sc} &= 0.341 + 0.341\mathbf{E} - 0.206\mathbf{S} - 0.024\mathbf{A} - 2.178\mathbf{B} + 1.850\mathbf{V} \\ &\left(N = 45,\ SD = 0.216,\ R^2 = 0.926,\ F = 97\right) \end{aligned} \tag{40}$$

based on an experimental database containing 45 solutes, including several linear alcohols (*e.g*. methanol through 1-decanol) and several fairly large steroidal molecules (*e.g*. testosterone, progesterone, hydrocortisone, corticosterone, and aldosterone) and steroid esters (*e.g*. hydrocortisone-21 acetate, hydrocortisone-21 pentanoate, cortisone-21 acetate, cortisone-21 octanoate). Careful examination of Eqn. 40 reveals that the water-to-skin partition coefficient increases with increasing solute size, and decreasing with increasing solute polarity and solute hydrogen-bonding character.

Abraham and Ibrahim (2007) compiled experimental data on the distribution coefficients of drugs from blood or plasma to rat skin and rabbit skin. The authors analyzed the experimental log P_{skin} data in accordance with Eqn. 1 of the Abraham model

$$\begin{aligned} \log P_{skin} &= -0.253 - 0.189\mathbf{A} - 0.620\mathbf{B} + 0.713\mathbf{V} - 0.683\mathbf{I}_{\mathbf{acid}} + 0.059\mathbf{I}_{\mathbf{rabbit}} \\ &\left(N = 59,\ SD = 0.26,\ R^2 = 0.733,\ F = 29\right) \end{aligned} \tag{41}$$

The e · **E** and s · **S** terms were not statistically significant and were eliminated from the final derived correlation model. The poor R^2 statistics for Eqn. 41 is due, at least in part, to the small spread in the values of log P_{skin}, from log P_{skin} = -0.82 to log P_{skin} = 1.61, for a range of only 2.43 log units. Carboxylic acids were found to be systematically retained in blood or plasma more than calculated. An indicator descriptor, $\mathbf{I_{acid}}$, was needed to describe the log Pskin data of solutes containing a carboxylic acid functional group. The $\mathbf{I_{acid}}$ descriptor equals unity for carboxylic acid solutes, and takes the value of $\mathbf{I_{acid}}$ = 0 for all other compounds. The second indicator descriptor in Eqn. 41 was needed to combine the rat skin ($\mathbf{I_{rabbit}}$ = 0) and rabbit skin ($\mathbf{I_{rabbit}}$) partitioning data into a single correlation model. The 0.059 $\mathbf{I_{rabbit}}$ term amounts to a 0.059 log unit offset, which is likely less than the experimental uncertainty in the measured log P_{skin} data. If the 0.059 $\mathbf{I_{rabbit}}$ term is omitted, the squared correlation coefficient decreases to R^2 = 0.608.

Theoretical models of passive diffusion are based on Fick's law of diffusion and the conversation of particle numbers. Fick's law of diffusion states that a chemical diffuses from a region of higher concentration to a region of lower concentration with a magnitude that is directly proportional to the chemical's concentration gradient. When applied to trans-stratum corneum diffusion, the amount of chemical passing through a unit area of the stratum corneum per unit time (J) is given by

$$J = -\frac{K_{p,sc} D \Delta C}{h} \tag{42}$$

where $K_{p,sc}$ is the chemical's solvent-to-stratum corneum partition coefficient, D represents the chemical's diffusivity in the stratum corneum lipid matrix and h is the apparent skin thickness (*i.e.*, the diffusion pathlength). Under the assumption of constant donor concentration and sink conditions (zero receptor phase concentration) Eqn. 42 simplifies to

$$J_{SS} = \frac{K_{p,sc} D C_{donor}}{h} \tag{43}$$

The permeability coefficient, k_p, is the coefficient of proportionality between the steady-state flux J_{SS} and the donor concentration, C_{donor}.

Skin permeability experiments are generally performed *in vitro* using a Franz diffusion cell (shown in Figure 8). A freshly excised skin sample is mounted on the receptor compartment of the Franz cell with the stratum corneum facing upwards into the donor compartment and the dermis facing the receptor compartment. The latter compartment is filled with the receptor solution (often a phosphate saline solution buffered at pH of 7.4), and maintained at a constant temperature of 37 °C with a water jacketed cell under constant stirring. The donor compartment is filled with the vehicle solution containing the dissolved chemical of interest. At appropriate time intervals, aliquots of the receptor medium are withdrawn for analysis, and immediately replaced with an equal volume of fresh medium. Alternative diffusion cell designs and mathematical procedures for calculating the drug's diffusivity and permeability coefficient from the experimental permeation results are described in greater detail elsewhere (Friend, 1992; Hathout *et al.*, 2010). For *in vitro* skin penetration studies, the skin retention of a drug can be assessed by the use of radiolabeled drugs (usually carbon-14 or tritium labeled). Skin samples should be exposed to the drug for no more than a maximum of 24 hours because of deterioration of skin integrity with time.

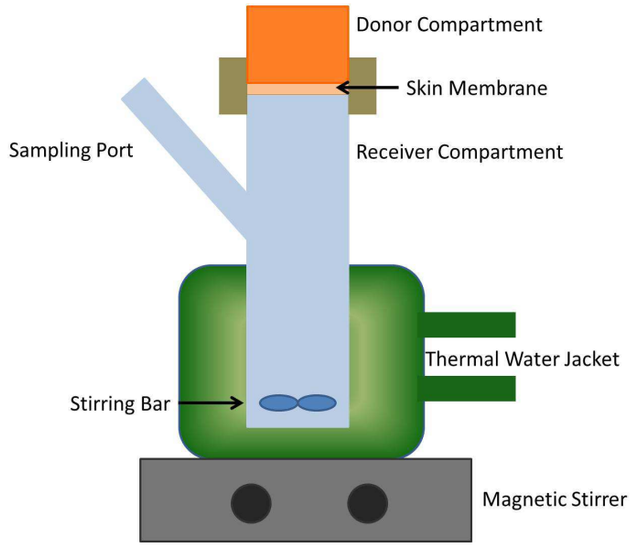

Fig. 8. Franz diffusion cell used to measure skin permeability coefficients

The parallel artificial membrane permeability assay (PAMPA) has been suggested as a high throughput screening method for rapid determination of passive transport permeability in connection with gastrointestinal (GI) absorption (Sugano *et al*., 2002), blood-brain barrier penetration (Mensch *et al*., 2010 and skin permeation (Ottaviani *et al*., 2006). In the PAMPA method a 96-well filter plate coated with a liquid membrane is used to separate the donor and receptor compartments. Artificial membrane selection depends on the transport property to be determined. Ottaviani *et al*. (2006) found a reasonably accurate mathematical correlation between human skin permeability coefficient, k_p, and the effective permeability coefficient, k*eff*, for a set of 31 compounds

$$\log k_p = 1.34 \log k_{eff} + 0.28 \quad (N = 31,\ SD = 0.42,\ R^2 = 0.81,\ F = 31) \tag{44}$$

tested through an artificial membrane consisting of 70 % silicone and 30 % isopropyl myristate. The authors further noted that presence of isopropyl myristate as only a hydrogen-bond acceptor group in the artificial membrane was in accord with previous results demonstrating that stratum corneum lipids were better hydrogen-bond acceptors than hydrogen-bond donors.

Abraham and Martins (2004) reported an Abraham model correlation for human skin permeability coefficients from aqueous solution, k_p,

$$\text{Log}\, k_p(\text{cm/s}) = -5.426 - 0.106\mathbf{E} - 0.473\mathbf{E} - 0.473\mathbf{A} - 3.000\mathbf{B} + 2.296\mathbf{V} \quad \left(N = 119,\ SD = 0.461,\ R^2 = 0.832,\ F = 112\right) \tag{45}$$

based on a database containing 119 experimental values at a common temperature of 37 ^{o}C. The authors adjusted the experimental data for ionization by assuming that the measured permeability coefficient was a simple addition of terms in Eqn. 46

$$k_p = f_{neutral}\, k_{p,neutral} + f_{ionic} k_{p,ionic} \tag{46}$$

where, k_p, $k_{p,ionic}$, and $k_{p,neutral}$ represent the overall permeation coefficient, that due to the ionic species, and that due to the neutral species; f_{ionic} and $f_{neutral}$ denote the fraction of ionic and neutral species at a given pH. For ionizable acids the skin permeability coefficient of the neutral molecule, $k_{p,neutral}$, was so much larger than the skin permeability coefficient of the ionic form, $k_{p,ionic}$, that the experimental unadjusted values of k_p was adjusted to give $k_{p,neutral}$ from the fraction of the neutral form present under the experimental conditions of pH. For ionizable bases the ratio of $k_{p,neutral}$ to $k_{p,ionic}$ was assumed to be 17.5, and this value was used to obtain $k_{p,neutral}$ values from experimental unadjusted values of k_p. If the experimental pH is near to the basic pK_a, such an adjustment will be very close to the adjustment that assumes negligible permeation of ionizable species. But as the difference in $(pH - pK_a)$ becomes larger, the adjustment will be smaller than that of negligible permeation of ionic species. To account for the temperature differences, the authors adjusted experimental log k_p values by 0.20 units from 32 °C to 37 °C, and by 0.48 units from 25 °C to 37 °C. The main factors that influence log k_p are hydrogen bond basicity ($b \cdot B$ term) that decreases log k_p, and solute volume ($v \cdot \mathbf{V}$ term) that increases log k_p. Solute dipolarity/polarizability ($s \cdot S$ term) and hydrogen bond acidity ($a \cdot \mathbf{A}$ term) make minor contributions, both in the sense of lowering log k_p.

9. Conclusion

The Abraham solvation parameter model provides an in silico method for estimating ADMET properties of potential drug molecules in the early stages of drug discovery. To date mathematical expressions have been reported for predicting water-to-organic solvent partition coefficients and solubilities in more than 70 organic solvents, air-to-tissue and blood-to-tissue partition coefficients for 5 human and rat tissues, water-to-human skin and blood-to-rat/rabbit skin partitions, human skin permeability coefficients, and rat (Zhao *et al*., 2003) and human (Zhao *et al*., 2002) intestinal absorption. Expressions are also available for estimating Draize rabbit eye test scores for pure liquids and eye irritation thresholds in humans (Abraham *et al*., 2003), odor detection thresholds and nasal pungency of volatile organic compounds (VOCs) (Abraham *et al*., 2007b), and the minimum alveolar concentration (MAC) for inhalation anesthetics in rats (Abraham *et al*., 2008b). The number of derived Abraham model correlations is expected in future years as more experimental data becomes available. Predictive applications require as input parameters the numerical values of the drug candidate's solute descriptors, which are easily calculable from measured solubility and partition coefficient data.

10. References

Abraham, M. H. & McGowan, J. C. (1987) The use of characteristic volumes to measure cavity terms in reversed phase liquid chromatography. *Chromatographia* 23 (4) 243–246.

Abraham, M. H. (1993a) Scales of solute hydrogen-bonding: their construction and application to physicochemical and biochemical processes. *Chemical Society Reviews* 22 (2),73-83.

Abraham, M. H. (1993b) Application of solvation equations to chemical and biochemical processes. *Pure and Applied Chemistry* 65 (12), 2503-2512.

Abraham, M. H.; Hassanisadi, M.; Jalali-Heravi, M.; Ghafourian, T.; Cain, W. S. & Cometto-Muniz, J. E. (2003) Draize rabbit eye test compatibility with eye irritation thresholds

in humans: a quantitative structure-activity relationship analysis. *Toxicological Sciences* 76 (2), 384-391.

Abraham, M. H. (2004) The factors that influence permeation across the blood-brain barrier. *European Journal of Medicinal Chemistry* 39 (3), 235-240.

Abraham, M. H.; Ibrahim, A. & Zissimos, A. M. (2004) Determination of sets of solute descriptors from chromatographic measurements. *Journal of Chromatography, A* 1037 (1-2), 29-47.

Abraham, M. H. & Martins, F. (2004) Human skin permeation and partition: General linear free-energy relationship analyses. *Journal of Pharmaceutical Sciences* 93 (6), 1508-1523.

Abraham, M. H.; Ibrahim, A. & Acree, W. E. Jr., (2005) Air-to-blood distribution of volatile organic compounds: a linear free energy analysis. *Chemical Research in Toxicology* 18 (5), 904-911.

Abraham, M. H. & Ibrahim, A. (2006) Air to fat and blood to fat distribution of volatile organic compounds and drugs: Linear free energy analyses. *European Journal of Medicinal Chemistry* 41 (12), 1430-1438.

Abraham, M. H.; Ibrahim, A. & Acree, W. E (2006a) Air to brain, blood to brain and plasma to brain distribution of volatile organic compounds: linear free energy analyses. *European Journal of Medicinal Chemistry* 41 (4), 494-502.

Abraham, M. H.; Ibrahim, A.; Zhao, Y. & Acree, W. E., Jr. (2006b) A data base for partition of volatile organic compounds and drugs from blood/plasma/serum to brain, and an LFER analysis of the data. *Journal of Pharmaceutical Sciences* 95 (10), 2091-2100.

Abraham, M. H.; Ibrahim, A. & Acree, W. E., Jr. (2006c) Air to muscle and blood/plasma to muscle distribution of volatile organic compounds and drugs: linear free energy analyses. *Chemical Research in Toxicology* 19 (6), 801-808.

Abraham, M. H. & Ibrahim, A. (2007) Blood or plasma to skin distribution of drugs: a linear free energy analysis. *International Journal of Pharmaceutics* 329 (1-2) 129-134.

Abraham, M. H.; Ibrahim, A. & Acree, W. E., Jr. (2007a) Air to liver partition coefficients for volatile organic compounds and blood to liver partition coefficients for volatile organic compounds and drugs. *European Journal of Medicinal Chemistry* 42 (6), 743-751.

Abraham, M. H.; Sanchez-Moreno, R.; Cometto-Muniz, J. E. & Cain, W. S. (2007b) A quantitative structure-activity analysis on the relative sensitivity of the olfactory and the nasal trigeminal chemosensory systems. *Chemical Senses* 32 (7), 711-719.

Abraham, M. H.; Ibrahim, A. & Acree, W. E, Jr. (2008a) Air to lung partition coefficients for volatile organic compounds and blood to lung partition coefficients for volatile organic compounds and drug. *European Journal of Medicinal Chemistry* 43 (3), 478-485.

Abraham, M. H.; Acree, W. E., Jr.; Mintz, C. & Payne, S. (2008b) Effect of anesthetic structure on inhalation anesthesia: implications for the mechanism. *Journal of Pharmaceutical Sciences* 97 (6), 2373-2384.

Abraham, M. H.; Acree, W. E., Jr. & Cometto-Muniz, J. E. (2009a) Partition of compounds from water and from air into amides. *New Journal of Chemistry* 33 (10), 2034-2043.

Abraham, M. H.; Gil-Lostes, J. & Fatemi, M. (2009b) Prediction of milk/plasma concentration ratios of drugs and environmental pollutants. *European Journal of Medicinal Chemistry* 44 (6), 2452-2458.

Abraham, M. H. & Acree, W. E., Jr. (2010a) Equations for the transfer of neutral molecules and ionic species from water to organic phases. *Journal of Organic Chemistry* 75 (4), 1006-1015.

Abraham, M. H. & Acree, W. E., Jr. (2010b) Solute descriptors for phenoxide anions and their use to establish correlations of rates of reaction of anions with iodomethane. *Journal of Organic Chemistry* 75 (9), 3021-3026.

Abraham, M. H. & Acree, W. E., Jr. (2010c) The transfer of neutral molecules, ions and ionic species from water to ethylene glycol and to propylene carbonate; descriptors for pyridinium cations. *New Journal of Chemistry* 34 (10), 2298-2305.

Abraham, M. H. & Acree, W. E., Jr. (2010d) The transfer of neutral molecules, ions and ionic species from water to wet octanol. *Physical Chemistry Chemical Physics* 12 (40), 13182-13188.

Abraham, M. H.; Smith, R. E.; Luchtefeld, R.; Boorem, A. J.; Luo, R. & Acree, W. E., Jr. (2010) Prediction of solubility of drugs and other compounds in organic solvents. *Journal of Pharmaceutical Sciences* 99 (3), 1500-1515.

Abraham, M. H. (2011) The permeation of neutral molecules, ions and ionic species: brain permeation as an example. *Journal of Pharmaceutical Sciences*, 100, (5), 1690-1701.

Acree, W. E., Jr. & Abraham, M. H. (2002) Solubility of crystalline nonelectrolyte solutes in organic solvents: mathematical correlation of benzil solubilities with the Abraham general solvation model. *Journal of Solution Chemistry* 31 (4), 293-303

ADME Boxes, version*, Advanced Chemistry Development, 110 Yonge Street, 14th Floor, Toronto, Ontario, M5C 1T4, Canada.

Ahmed, H.; Poole, C. F. & Kozerski, G. E. (2007) Determination of descriptors for organo-silicon compounds by gas chromatography and non-aqueous liquid-liquid partitioning. *Journal of Chromatography, A* 1169 (1-2), 179-192.

Ahmed, H. & Poole, C. F. (2006a) Distribution of neutral organic compounds between n-heptane and methanol or N,N-dimethylformamide. *Journal of Separation Science* 29 (14), 2158-2165.

Ahmed, Hamid & Poole, Colin F. (2006b) Model for the distribution of neutral organic compounds between n-hexane and acetonitrile. *Journal of Chromatography, A* 1104 (1-2), 82-90.

Alam, M. I.; Beg, S.; Samad, A.; Baboota, S.; Hohli, K.; Ali, J.; Ahuja, A. & Akbar, M. (2010) Strategy for effective brain drug delivery. *European Journal of Pharmaceutical Science* 40 (5), 385-403.

Amidon, G. L.; Lennenas, H.; Shah, V. P. & Crison, J. R. (1995) A theoretical basis for a biopharmaceutic drug classification: the correlation in vitro drug product dissolution and in vivo bioavailability. *Pharmaceutical Research* 12 (3), 413-420.

Arey, J. S.; Green, W. H., Jr. & Gschwend, P. M. (2005) The electrostatic origin of Abraham's solute polarity parameter. *Journal of Physical Chemistry B* 109 (15), 7564-7573.

Atapattu, S. N. & Poole, C. F. (2009) Determination of descriptors for semivolatile organosilicon compounds by gas chromatography and non-aqueous liquid-liquid partition. *Journal of Chromatography, A* 1216 (45), 7882-7888.

Begley, D. J.; Khan, E. U.; Rollinson, C. & Abbott, J. (2000) in 'The blood-brain barrier and drug delivery to the CNS, Ed by Befley, D.J.; Bradbury, M. W. & Kreuter, J., Marcel Dekker, New York, 2000.

Berthod, A.; Han, Y. Il. & Armstrong, D. W. (1988) Centrifugal partition chromatography. V. Octanol-water partition coefficients, direct and indirect determination. *Journal of Liquid Chromatography* 11 (7), 1441-1456.

Berthod, A.; Menges, R. A. & Armstrong, D. W. (1992) Direct octanol-water partition coefficient determination using co-current chromatography. *Journal of Liquid Chromatography* 15 (15-16), 2769-2785.

Charlton, A. K.; Daniels, C. R.; Acree, W. E., Jr. & Abraham, M. H. (2003) Solubility of crystalline nonelectrolyte solutes in organic solvents: mathematical correlation of acetylsalicylic acid solubilities with the Abraham general solvation model. *Journal of Solution Chemistry* 32 (12), 1087-1102.

Cruciani, G.; Pastor, M. & Guba, W. (2000) VolSurf: a new tool for the pharmacokinetic optimization of lead compounds. *European Journal of Pharmaceutical Sciences* 11 (Suppl. 2), S29-S39.

Eixarch, H.; Haltner-Ukomadu, E.; Beisswenger, C. & Bock, U. (2010) Drug delivery to the lung: permeability and physicochemical characteristics of drugs as the basis for a pulmonary Biopharmaceutical Classification System (pBCS). *Journal of Epithelial Biology and Pharmacology* 3, 1-14.

Faller, B.; Grimm, H. P.; Loeuillet-Ritzler, F.; Arnold, S. & Briand, X. (2005) High-throughput lipophilicity measurement with immobilized artificial membranes. *Journal of Medicinal Chemistry* 48 (7), 2571-2576.

Friend, D. R. (1992) *In vitro* skin permeation techniques. *Journal of Controlled Re*lease 18, 235-248.

Gao, X.; Yu, C. H.; Tam, K. Y. & Tsang, S. C. (2005) New magnetic nano-absorbent for the determination of n-octanol/water partition coefficients. *Journal of Pharmaceutical and Biomedical Analysis* 38 (2), 197-203.

Guthrie J. P. (2009) A blind challenge for computational solvation free energies: introduction and overview. *Journal of Physical Chemistry B* 113 (14) 4501-4507.

Hathout, R. M.; Woodman, T. J.; Mansour, S.; Mortada, N. D.; Geneidi, A. S. & Guy, R. H. (2010) Microemulsion formulations for the transdermal delivery of testosterone. *European Journal of Pharmaceutical Sciences* 40 (3), 188-196.

Henchoz, Y.; Romand, S.; Schuppler, J.; Rudaz, S.; Veathey, J.-L. & Carrupt, P. A. (2010) High-throughput log P determination by MEEKC coupled with UV and MS detections. *Electrophoresis*, 31 (5), 952-964.

Hewitt, M.; Cronin, M. T. D.; Enoch, S. J.; Madden, J. C.; Roberts, D. W. & Dearden, J. C. (2009) In silico prediction of aqueous solubility: the solubility challenge. *Journal of Chemical Information and Modeling* 49 (11), 2572–2587.

Holbrook K A. & Odland G F. (1974) Regional differences in the thickness (cell layers) of the human stratum corneum: an ultrastructural analysis. *The Journal of Investigative Dermatology* 62 (4), 415-422.

Howard, P. H. & Meylan, W. M. (1997) Handbook of Physical properties of Organic Chemicals, CRC Press, Boca Raton, 1997.

Ishihama, Y. & Asakawa, N. (1999) Characterization of the lipophilicity scales using vectors from solvation energy descriptors. *Journal of Pharmaceutical Sciences* 88 (12), 1305-1312.

Karunasekara, T. & Poole, C. F. (2010) Model for the partition of neutral compounds between n-heptane and formamide. *Journal of Separation Science* 33 (8), 1167-1173.

Keck, C.; Kobierski, S.; Mauludin, R. & Muller, R. H. (2008) Second generation of drug nanocrystals for delivery of poorly soluble drugs: smartcrystal technology. *Dosis*, 2 (24), 124-128 .

Li, H.; Yap, C. W.; Ung, C. Y.; Xue, Y.; Cao, Z. W. & Chen, Y. Z. (2005) Effect of selection of molecular descriptors on the prediction of blood-brain barrier penetrating and nonpenetrating agents by statistical learning methods. *Journal of Chemical Information and Modeling* 45 (5) 1376-1384.

Li, Q.-S.; Li, Z. & Wang, S. (2008) Solubility of trimethoprim (TMP) in different organic solvents from (278 to 333) K. *Journal of Chemical and Engineering Data* 53 (1), 286-287.

Lipinski, C. A.; Lombardo, F.; Dominy, B. W. & Feeney, P. J. (2001) Experimental and computational approaches to estimate solubility and permeability in drug discovery and development settings. *Advances in Drug Delivery Reviews* 46 (1-3), 3-26.

Llinàs, A.; Glen, R. C. & Goodman, J. M. (2008) Solubility challenge: can you predict solubilities of 32 molecules using a database of 100 reliable measurements. *Journal of Chemical Information and Modeling* 48 (7), 1289–1303.

Lukyanov, A. N. & Torchilin, V. P. (2004) Micelles from lipid derivatives of water-soluble polymers as delivery systems for poorly soluble drugs. *Advanced Drug Delivery Reviews* 56 (9), 1273-1289.

McDuffie, B. (1981) Estimation of octanol/water partition coefficients for organic pollutants using reverse-phase HPLC *Chemosphere* 10 (1), 73-83.

Menges, R. A.; Bertrand, G. L. & Armstrong, D. W. (1990) Direct measurement of octanolwater partition coefficients using centrifugal partition chromatography with a back-flushing technique. *Journal of Liquid Chromatography* 13 (15), 3061-3077.

Mensch, J.; Jaroskova, L.; Anderson, W.; Mells, A.; Mackle, C.; Verreck, G.; Brewster, M. E. & Augustinjns, P. (2010) Application of PAMPA-models to predict BBB permeability including efflux ratio, plasma protein binding and physicochemical parameters. *International Journal of Pharmaceutics* 395, 182-197.

Michaels A. S, Chandrasekaran S. K, & Shaw J. E. (1975).Drug permeation through human skin: theory and *in vitro* experimental measurement. *AIChE Journal* 21 (5), 985–996.

Mintz, C.; Clark, M.; Acree, W. E., Jr. & Abraham, M. H. (2007) Enthalpy of solvation correlations for gaseous solutes dissolved in water and in 1-octanol based on the Abraham model. *Journal of Chemical Information and Modeling* 47 (1), 115-121.

Monteiro-Riviere, N. A.; Inman, A. O.; Mak, V.; Wertz, P. & Riviere, J. E. (2001) Effect of selective lipid extraction from different body regions on epidermal barrier function. *Pharmaceutical Research* 18 (7) 992-998.

Mutelet, F. & Rogalski, M. (2001) Experimental determination and prediction of the gas-liquid n-hexadecane partition coefficients. *Journal of Chromatography A* 923 (102), 153-163.

Netzlaff, F.; Schaefer, U. F.; Lehr, C.-M.; Meiers, P.; Stahl, J.; Kietzmann, M. & Niedorf, F. (2006) Comparison of bovine udder skin with human and porcine skin in percutaneous permeation experiments. *ATLA, Alternatives to Laboratory Animals* 34 (5), 499-513.

Nicholls, A.; Mobley, D. L.; Guthrie, J. P.; Chodera, J. D.; Bayly, C. I.; Cooper, M. D. & Pande, V. S. (2008) Predicting small-molecule solvation free energies: an informal blind test for computational chemistry. *Journal of Medical Chemistry* 51 (4) 769-779.

Ottaviani, G.; Martel, S. & Carrupt, P.-A. (2006) Parallel artificial membrane permeability assay: A new membrane for the fast prediction of passive human skin permeability. *Journal of Medicinal Chemistry* 49 (6), 3948-3954.

Platts, J. A.; Butina, D.; Abraham, M. H. & Hersey, A. (1999) Estimation of molecular linear free energy relation descriptors using a group contribution approach. *Journal of Chemical Information and Computational Science* 39 (5), 835-845.

Poole, S. K. & Poole, C. F. (2003) Separation methods for estimating octanol-water partition coefficients. *Journal of Chromatographty B* 797 (1-2), 3-19.

Qian, J. & Poole, C. F. (2007) Distribution of neutral organic compounds between n-heptane and fluorine-containing alcohols. *Journal of Chromatography, A* 1143 (1-2), 276-283.

Ribeiro, M. M. B.; Melo, M. N.; Serrano, I. D.; Santos, N. C. & Castanho, M. A. R. B. (2010) Drug-lipid interaction evaluation: why a 19th century solution? *Trends in Pharmacological Sciences* 31 (10), 449-454.

Sangster, J. (1989) Octanol-water partition coefficients of simple organic compounds. *Journalof Physical and Chemical Reference Data* 18 (3), 1111-1229.

Sugano, K.; Takata, N.; Machida, M.; Saitoh, K. & Terada, K. (2002) Prediction of passive intestinal absorption using bio-mimetic artificial membrane permeation assay and the paracellular pathway. *International Journal of Pharmaceutics* 241 (2), 241-251

Sugano, K.; Kato, T.; Suzuki, K.; Keiko, K.; Sajaku, T. & Mano, T. (2006) High throughput solubility measurement with automated polarized light microscopy analysis. *Journal of Pharmaceutical Sciences* 95 (10), 2115-2122.

Veith, G. D.; Austin, N. M. & Morris, R. T. (1979) A rapid method for estimating log P for organic chemicals. *Water Research* 13 (1), 43-47

Wang, J. M.; Hou, T. J. & Xu, X. J. (2009) Aqueous solubility prediction based on weighted atom type counts and solvent accessible surface areas. *Journal of Chemical Information and Modeling* 49 (3), 571–581.

Wohnsland, F. & Faller, B. (2001) High-throughput permeability pH profile and high-throughput alkane/water log P with artificial membranes. *Journal of Medicinal Chemistry* 44 (6), 923-930.

Wu, C. Y. & Benet, L. Z. (2005) Predicting drug disposition via application of BCS. Transportabsorption/elimination interplay and development of a biopharmaceutics drug disposition classification system. *Pharmaceutical Research* 22 (1), 11-23.

Zhao, Y. H.; Le, J.; Abraham, M. H.; Hersey, A.; Eddershaw, P. J.; Luscombe, C. N.; Butina, D.; Beck, G.; Sherborne, B.; Cooper, I. & Platts, J. A. (2002) Evaluation of human intestinal absorption data and subsequent derivation of a quantitative structure-activity relationship (QSAR) with the Abraham descriptors. *Journal of Pharmaceutical Sciences* 90 (6), 749-784

Zhao, Y. H.; Abraham, M. H.; Hersey, A. & Luscombe, C. N. (2003) Quantitative relationship between rat intestinal absorption and Abraham descriptors. *European Journal of Medicinal Chemistry* 38 (11-12), 939-947.

Zhao, Y. H.; Abraham, M. H.; Ibrahim, A.; Fish, P. V.; Cole, S.; Lewis, M. L.; de Groot, M. J. & Reynolds, D. P. (2007) Predicting penetration across the blood-brain barrier from simple descriptors and fragmentation schemes. *Journal of Chemical Information and Modeling* 47 (1), 170-175.

Zissimos, A. M.; Abraham, M. H.; Barker, M. C.; Box, K. J.; & Tam, K. Y. (2002a) Calculation of Abraham descriptors from solvent-water partition coefficients in four different systems; evaluation of different methods of calculation. *Journal of the Chemical Society, Perkin Transactions 2* (3), 470-477.

Zissimos, A. M.; Abraham, M. H.; Du, C. M.; Valko, K.; Bevan, C.; Reynolds, D.; Wood, J.; & Tam, K. Y. (2002b) Calculation of Abraham descriptors from experimental data from seven HPLC systems; evaluation of five different methods of calculation. *Journal of the Chemical Society, Perkin Transactions 2* (12), 2001-2010.

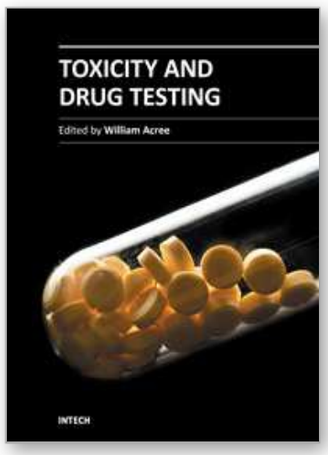

Toxicity and Drug Testing
Edited by Prof. Bill Acree

ISBN 978-953-51-0004-1
Hard cover, 528 pages
Publisher InTech
Published online 10, February, 2012
Published in print edition February, 2012

Modern drug design and testing involves experimental in vivo and in vitro measurement of the drug candidate's ADMET (adsorption, distribution, metabolism, elimination and toxicity) properties in the early stages of drug discovery. Only a small percentage of the proposed drug candidates receive government approval and reach the market place. Unfavorable pharmacokinetic properties, poor bioavailability and efficacy, low solubility, adverse side effects and toxicity concerns account for many of the drug failures encountered in the pharmaceutical industry. Authors from several countries have contributed chapters detailing regulatory policies, pharmaceutical concerns and clinical practices in their respective countries with the expectation that the open exchange of scientific results and ideas presented in this book will lead to improved pharmaceutical products.

How to reference
In order to correctly reference this scholarly work, feel free to copy and paste the following:

William E. Acree, Jr., Laura M. Grubbs and Michael H. Abraham (2012). Prediction of Partition Coefficients and Permeability of Drug Molecules in Biological Systems with Abraham Model Solute Descriptors Derived from Measured Solubilities and Water-to-Organic Solvent Partition Coefficients, Toxicity and Drug Testing, Prof. Bill Acree (Ed.), ISBN: 978-953-51-0004-1, InTech, Available from: http://www.intechopen.com/books/toxicity-and-drug-testing/prediction-of-partition-coefficients-and-permeability-of-drug-molecules-in-biological-systems-with-a

INTECH
open science | open minds

InTech Europe
University Campus STeP Ri
Slavka Krautzeka 83/A
51000 Rijeka, Croatia
Phone: +385 (51) 770 447
Fax: +385 (51) 686 166
www.intechopen.com

InTech China
Unit 405, Office Block, Hotel Equatorial Shanghai
No.65, Yan An Road (West), Shanghai, 200040, China
中国上海市延安西路65号上海国际贵都大饭店办公楼405单元
Phone: +86-21-62489820
Fax: +86-21-62489821

IntechOpen